

Cite this: *Biomater. Sci.*, 2024, **12**, 2203

## Emerging nanoparticle platforms for CpG oligonucleotide delivery

Mingqiang Li,<sup>†</sup> Haochen Yao,<sup>†</sup> Ke Yi,<sup>a</sup> Yeh-Hsing Lao,<sup>c</sup> Dan Shao<sup>d</sup> and Yu Tao<sup>id</sup> \*<sup>a</sup>

Unmethylated cytosine–phosphate–guanine (CpG) oligodeoxynucleotides (ODNs), which were therapeutic DNA with high immunostimulatory activity, have been applied in widespread applications from basic research to clinics as therapeutic agents for cancer immunotherapy, viral infection, allergic diseases and asthma since their discovery in 1995. The major factors to consider for clinical translation using CpG motifs are the protection of CpG ODNs from DNase degradation and the delivery of CpG ODNs to the Toll-like receptor-9 expressed human B-cells and plasmacytoid dendritic cells. Therefore, great efforts have been devoted to the advances of efficient delivery systems for CpG ODNs. In this review, we outline new horizons and recent developments in this field, providing a comprehensive summary of the nanoparticle-based CpG delivery systems developed to improve the efficacy of CpG-mediated immune responses, including DNA nanostructures, inorganic nanoparticles, polymer nanoparticles, metal–organic–frameworks, lipid-based nanosystems, proteins and peptides, as well as exosomes and cell membrane nanoparticles. Moreover, future challenges in the establishment of CpG delivery systems for immunotherapeutic applications are discussed. We expect that the continuously growing interest in the development of CpG-based immunotherapy will certainly fuel the excitement and stimulation in medicine research.

Received 2nd December 2023,  
Accepted 15th January 2024

DOI: 10.1039/d3bm01970e

rsc.li/biomaterials-science

### 1. Introduction

#### 1.1. A brief insight into the mechanism of CpG-induced immune activation

Investigation of cytosine–phosphate–guanine (CpG) oligodeoxynucleotides (ODNs) as therapeutic agents gained great attention since 1995 when Krieg *et al.* first discovered that CpG motifs in bacterial DNA could trigger the direct activation of B cells both *in vitro* and *in vivo*.<sup>1</sup> Five years later, Hemmi *et al.* published their celebrated proof-of-principle experiment elucidating the mechanism of CpG activation.<sup>2</sup> Unmethylated CpG ODNs, which are frequent in the genomes of bacteria but rare in vertebrate genomes,<sup>3</sup> are able to activate the immune system and thus have shown great potential for the therapy of a wide variety of diseases, such as infection, allergies, asthma

and cancer.<sup>4–13</sup> Extensive basic research, as well as clinical trials, provides significant evidence of translational potential of using CpG ODNs as therapeutics.<sup>14</sup> Discussion of CpG ODNs for the prophylaxis or treatment of tumors, allergies, and infectious diseases can be found in several reviews published in the last decade.<sup>15–23</sup> CpG ODNs are known ligands for Toll-like receptor (TLRs)-9 (TLR9), which are loaded within the endosomal compartment in the B cell and plasmacytoid dendritic cell (pDC) intracellular compartments.<sup>24–26</sup> TLRs are a family of pattern recognition receptors composed of a cytoplasmic Toll/interleukin-1 receptor area and an extracellular leucine-rich repeat, connecting through a transmembrane domain.<sup>27</sup> TLRs consist of ten different TLR subtypes (TLR1 to TLR10), among which TLR9 plays a critical role in CpG ODN-induced immunostimulation (Fig. 1).<sup>28–31</sup> Binding of CpG ODNs to TLR9 dimers results in allosteric changes of TLR9 cytoplasmic signaling domains, leading to signaling adaptor molecule recruitments.<sup>32</sup> TLR9 combines with myeloid differentiation factor 88 (MyD88) to activate CpG-mediated effects *via* signal-transducing proteins, including mitogen-activated kinases or interferon (IFN) regulatory factors, members of the interleukin (IL)-1 receptor-associated kinase (IRAK) family.<sup>33–35</sup> These result in nuclear factor-kappa B (NF-κB) transcription factor activations, cytokine productions or co-stimulatory molecule expressions in human B cells and pDCs.<sup>36,37</sup> CpG

<sup>a</sup>Laboratory of Biomaterials and Translational Medicine, Center for Nanomedicine, The Third Affiliated Hospital, Sun Yat-sen University, Guangzhou 510630, China. E-mail: taoy28@mail.sysu.edu.cn

<sup>b</sup>Hepatobiliary and Pancreatic Surgery Department, General Surgery Center, First Hospital of Jilin University, No. 1 Xinmin Street, Changchun, 130021 Jilin, China

<sup>c</sup>Department of Pharmaceutical Sciences, University at Buffalo, The State University of New York, Buffalo, NY, 14214, USA

<sup>d</sup>Institutes of Life Sciences, School of Biomedical Sciences and Engineering, South China University of Technology, Guangzhou, China

<sup>†</sup>These authors contributed equally.

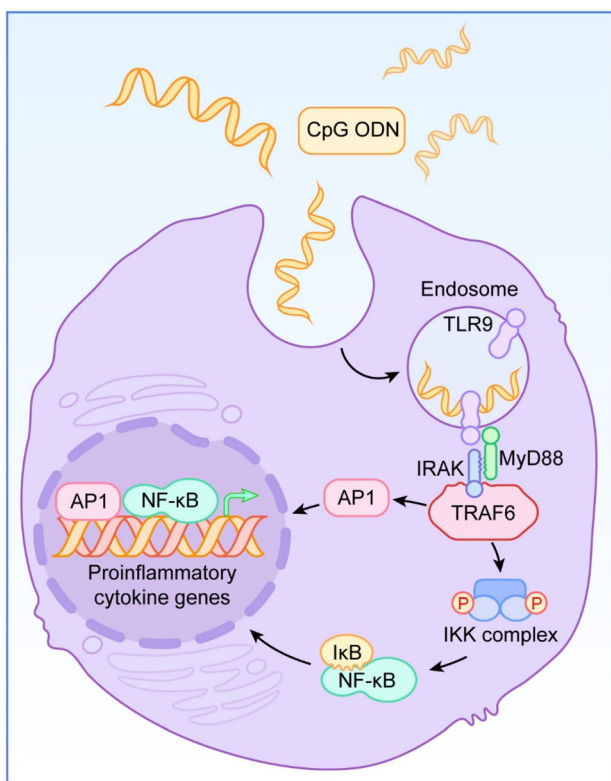


**Fig. 1** Schematic illustration of CpG ODN–TLR9 cell signaling. CpG ODNs enter into endosomal vesicles containing TLR9 receptors. The interaction between CpG ODNs and TLR9 triggers an intracytoplasmic activation signal. This signaling cascade begins with the recruitment of the myeloid differentiation primary response gene 88 (MyD88) to the Toll/interleukin-1 receptor domain of TLR9. Subsequently, the IL-1 receptor-activated kinase (IRAK) and tumor-necrosis factor receptor-associated factor 6 (TRAF6) complex becomes activated. This activation leads to the stimulation of inhibitor of nuclear factor- $\kappa$ B (NF- $\kappa$ B) kinase (IKK) complexes, ultimately resulting in the upregulation of transcription factors, including NF- $\kappa$ B and activating protein-1 (AP1).

motifs, as immunotherapeutic adjuvants,<sup>38,39</sup> can also enhance antigen presentation,<sup>40</sup> trigger immunostimulatory responses that induce the proliferation, maturation, and differentiation of various immune cells (e.g. natural killer cells, T and B lymphocytes, macrophages), as well as increase cytokine productions (e.g. interleukin-6 (IL-6), interleukin-10 (IL-10), interleukin-12 (IL-12), tumor necrosis factor- $\alpha$  (TNF- $\alpha$ ), interferon- $\alpha$  (IFN- $\alpha$ ), and interferon- $\gamma$  (IFN- $\gamma$ )).<sup>41,42</sup> As a result, CpG ODNs can be applied either as stand-alone molecules or as adjuvants to other therapies.<sup>25</sup>

To date, four different categories of CpG ODNs, based on their differences in sequences, secondary structures, and immune effects,<sup>16</sup> have been explored (Table 1): the A-, B-, C- and P-type CpG ODNs.<sup>43,44</sup> A-type (also known as D-type) CpG ODN is characterized by the palindromic structure composed of poly G motifs with a phosphorothioate (PS) backbone at each end and phosphodiester backbone at the sequencing center.<sup>45,46</sup> The PS modification is able to protect the CpG ODNs against DNase degradation,<sup>47</sup> and the poly G tails form intermolecular tetrads that lead to high molecular weight aggregates, which enhance cellular uptake. Although this type of CpG activates the TLR9 of pDCs and elicits IFN- $\alpha$ , it rarely induces B cell multiplication.<sup>3</sup> B-type (also known as K-type) contains a linear structure consisting entirely of a PS backbone.<sup>48,49</sup> B-type CpG triggers the activation and proliferation of B cells, but it shows a poor ability to induce IFN- $\alpha$  with pDCs.<sup>50</sup> C-type CpG includes not only a PS bridge but also the CpG motif and the palindrome linked by phosphodiester bonds. This class of CpG ODN, with an immunostimulatory quality between the A and B classes, exhibits the capabilities to induce the IFN- $\alpha$  production of pDCs and B cell proliferation.<sup>51,52</sup> Lastly, the P-type CpG ODNs, which have two palindromic motifs on their phosphorothioate backbones, possess high ability for IFN- $\alpha$  production and NF- $\kappa$ B activation.<sup>53</sup>

## 1.2. The advantages of CpG nanomedicine

In recent years, nanoparticle (NP)-mediated delivery has emerged as a new direction to deliver CpG ODNs (Fig. 2). Naked CpG ODNs are susceptible to nuclease degradation, which limits their half-life. Moreover, to be effective, CpG ODNs need to be delivered to the cytoplasm of the cells, thus requiring cell internalization and endosomal escape. Therefore, incorporating or conjugating CpG ODNs into or onto NPs engenders a number of potential advantages to maximize the immune responses, which, depending on the NP and the formulation parameters, include controlling the pharmacokinetics of CpG ODNs, protecting CpG ODNs from premature degradation, increasing the accumulation of the drug at the target site, enhancing uptake into target cells, and providing an opportunity for the co-delivery of allergen/antigen and CpG ODNs to the same antigen-presenting cells (APCs). The advantages of NP-based CpG delivery include: (1) protection of CpG ODNs from DNase degradation; (2) improved cellular uptake of CpG ODNs; (3) extended circulation lifetime of CpG ODNs inside the body; and (4) targeted delivery of CpG ODNs



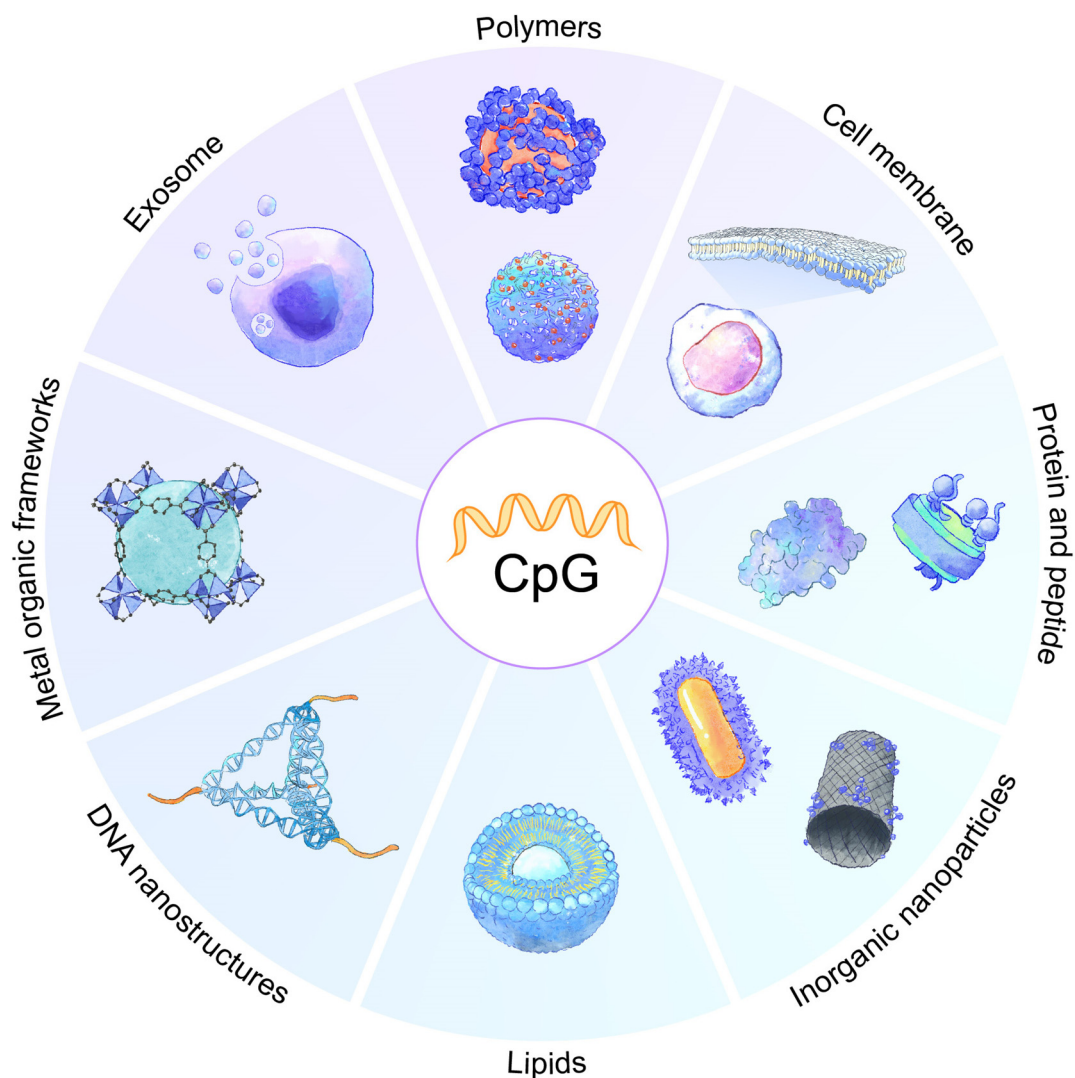
**Yu Tao**

*Dr Yu Tao is a professor at Sun Yat-sen University. She received her PhD degree in Inorganic Chemistry and Chemical Biology from Changchun Institute of Applied Chemistry, Chinese Academy of Sciences in 2015. Afterwards, she completed her postdoctoral training at the City College of New York and Columbia University from 2015 to 2018. Dr Tao has published more than 70 peer-reviewed papers as the first and corresponding author.*

*Her research interests include biomaterials, nanotechnology, and tissue engineering.*

**Table 1** Properties of different types of CpG ODN

Types	Sequences	Mainly stimulated cell types	Functions
Type-A (type-D)	ODN1585: 5'-GGGGTCAACGTTGAGGGGGG-3' ODN2216: 5'-GGGGGACGATCGTCGGGGG-3' ODN2336: 5'-GGGGACGACGTCGTGGGGGG-3'	pDCs	TNF- $\alpha$ , IFN- $\alpha$ , IL-12, IP10 secretion
Type-B (type-K)	ODN1668: 5'-TCCATGACGTTCTGTGCT-3' ODN1826: 5'-TCCATGACGTTCTGTGACGTT-3' ODN2006 (ODN 7909): 5'-TCGTGTTTTGTCGTTTTGTCGTT-3' ODN2007: 5'-TCGTGTTGTCGTTTTGTCGTT-3' ODN BW006: 5'-TCGACGTTTCGTTTCGTCGTTTC-3' ODN D-SL01: 5'-TCGCGACGTTTCGCCCGACGTTTCGGTA-3'	B-cells	IL-6, IL-10, IL-12 secretion; antibody production
Type-C	ODN2395: 5'-TCGTGTTTTTCGGCGCGCGCCG-3' ODN M362: 5'-TCGTGTCGTTTCGAACGACGTTGAT-3' ODN D-SL03: 5'-TCGCGAACGTTTCGCCCGGTTTCGAACGCGG-3'	pDCs; B-cells	Intermediate between types-A and -B
Type-P	ODN21798: 5'-TCGTGACGATCGGCCGCGCGCCG-3'	pDCs	Higher IFN- $\alpha$ secretion than type-C CpG

**Fig. 2** Schematic illustration of different carriers for CpG delivery.

to specific tissues with the help of modified NPs.<sup>54</sup> Therefore, with a wide spectrum of NP systems, it is expected that the delivery efficacy and immune activation of CpG ODNs can be substantially enhanced. The development of nanotechnology for CpG delivery has only recently started, but is occurring at a fast pace due to inspiration and adaptation from successes in the treatments of various disease targets. This review presents a comprehensive overview of NP-based CpG delivery systems that are being developed to enhance the efficacy of CpG ODN-mediated immune responses. Both *in vitro* and *in vivo* experiments suggested that such NP-based CpG delivery systems exhibited significant potential in human medicine. Considerable attention is paid to the synthesis and design of powerful nanoformulations that facilitate CpG delivery. In particular, we also discuss novel nanoplatforms that co-delivered antigen and CpG ODNs, and multifunctional nanoparticles that combined CpG-based immunotherapy with other treatment modalities. Additionally, we provide a brief outlook on current challenges and speculate the future direction of nanomaterial-based CpG delivery systems.

## 2. DNA nanostructure-based CpG delivery

Through the design of Watson–Crick base-pairing, DNA has been proved as a powerful scaffold to establish molecularly accurate designer DNA nanodevices.<sup>55</sup> Benefitting from high biocompatibility and excellent structural programmability, self-assembled DNA nanostructures have emerged as promising candidates to serve as efficient nanocarriers for drug delivery.<sup>56–59</sup> Recent research has indicated that DNA nanocarriers can also be efficiently utilized for CpG delivery.<sup>21,60</sup> In the design of the DNA nanostructures, the secondary structure of CpG ODNs is an important factor influencing the immune response. 5'-Terminal secondary structures showed greater influence on the immunostimulatory activity than those at the 3'-end.<sup>61</sup> Specifically, the immune function of CpG ODNs is minimized greatly in the presence of secondary structures at the 5'-end flanking sequence. The demand for an open 5'-end indicates that the receptor responsible for immune stimulation reads CpG ODNs from this end. Recent research suggested that nonmodified CpG ODNs with nuclease-resistant G-quadruplex structures had a greater advantage in terms of increasing the expression of IL-6, which could contribute to efficient CpG transport into endosomes by improving the cellular uptake and stability of nucleotides.<sup>62</sup> A lot of different DNA nanostructures have been applied for CpG transportation, such as polypod-like DNA, dendrimer-like DNA, DNA tetrahedra, DNA origami, DNA particles based on rolling circle amplification, and DNA hydrogel.

### 2.1. Polypod-like DNA nanostructures

Polypod-like DNA nanostructure-based CpG delivery platforms have been well established. The DNA polypod nanoassemblies were designed in polypod-like structures consisting of

different numbers of CpG motifs. The polypod-like CpG DNA can be used to investigate the systematic information on the relationship between the design and structural and biological properties of such branched DNA assemblies, providing a new approach to increasing the potency of CpG DNA as an adjuvant. Nishikawa's group has conducted a series of works in the area of DNA assembly-based CpG delivery. In 2008, Nishikawa and Takakura prepared Y-shaped CpG ODNs using three ODNs. These Y-shaped CpG ODNs stimulated larger amounts of IL-6 and TNF- $\alpha$  from macrophage cells than conventional single- and double-stranded CpG.<sup>63</sup> Furthermore, the same group reported on the polypod-like DNA structures containing CpG motifs. DNA nanoassemblies composed of three to eight pods were synthesized, with sizes of about 10 nm in diameter. Among them, polypodna with six or eight pods induced greater secretion of TNF- $\alpha$  and IL-6 from RAW264.7 cells.<sup>64</sup> Moreover, the immune activity of polypod-like CpG nanostructures was also evaluated *in vivo*, which was consistent with the *in vitro* result indicating that CpG-hexapodna induced high plasma IL-12p40 production.<sup>65</sup> In addition, Caruso and colleagues developed DNA microcapsules made of >4 million copies of Y-shaped CpG arranged into 3D nanostructures to enhance the immunostimulatory activity and serum stability of CpG. The nanocapsules stimulated up to 20-fold and 10-fold enhancements in proinflammatory cytokine IL-6 and TNF- $\alpha$  secretion in macrophage cells as compared with CpG alone.<sup>66</sup> Recently, Caruso's group synthesized uniform DNA-based particles with different morphologies *via* the supramolecular assembly of different DNA building blocks (plasmid DNA and Y-shaped DNA) and tannic acid (Fig. 3A). The particles enabled the efficient codelivery of CpG and the antigen ovalbumin, which could act as vaccines by inducing a good level of antibody production and T-cell responses.<sup>67</sup>

### 2.2. Dendrimer-like DNA nanostructures

Dendrimer-like DNA nanostructures, by connecting Y-shaped DNA that is composed of three short DNAs, with attractive characteristics including high biocompatibility, customized sizes, and excellent mechanical stability, are appealing for CpG delivery applications. Nishikawa's group designed dendrimer-like DNA through Y-DNA monomer ligase. The dendrimer-like CpG ODNs were effective in inducing greater amounts of the proinflammatory cytokines IL-6 and TNF- $\alpha$  in TLR9-positive macrophage cells as compared with conventional CpG or with its component Y-shaped CpG, suggesting that the formation of a dendritic structure can potentially increase the immune activity of CpG ODNs.<sup>68</sup> In addition, self-assembled CpG dendrimers could also be fabricated through the facile annealing procedure of properly designed ODNs without the DNA ligase process. These complicated CpG dendrimers were very effective in inducing the release of TNF- $\alpha$  from RAW264.7 cells.<sup>69</sup> Recently, CpG DNA dendrimeric nanoparticles were also modified with TAT peptide to further enhance cell internalization and immune responses.<sup>70</sup> In order to study the structure–function relationship that dominates vaccine activity, Mirkin's group also utilized DNA dendrons as the delivery



hedra vehicle to potentiate immuno-chemotherapy, in which the CpG ODNs and immunogenic cell death-inducers acted as an adjuvant to enhance the immunotherapy and doxorubicin employed as the chemotherapy drug.<sup>79</sup> Similarly, Liu's group lately developed skin-penetrating DNA tetrahedra to transdermally deliver the chemotherapeutic agent doxorubicin into melanoma to trigger the immunogenic death of tumor cells and expose tumor antigens, which with the aid of CpG ODNs incorporated in the DNA tetrahedra could stimulate systemic tumor-specific immune activities for efficient non-invasive skin cancer therapy (Fig. 3B).<sup>80</sup>

#### 2.4. DNA origami

DNA origami applies various short 'staple' strands to hybridize with domains on the viral-genome-derived DNA scaffold, folding it into accurate super architectures.<sup>55,81</sup> Compared with other DNA nanostructures, DNA origami can precisely regulate the number and location of CpG ODNs, and can effectively prevent the enzymatic degradation of CpG. Liedl and Bourquin measured the immune response triggered by hollow DNA origami tubes linked with 62 CpG sequences.<sup>82</sup> The DNA origami functionalized with CpG overhangs activated a strong immune response, characterized by the production of IL-6 and IL-12p70 cytokines and the activation of immune cells. These decorated origami tubes could trigger higher immunostimulation levels than the Lipofectamine-CpG system. After that, Bastings's group also studied the effects of spatial patterns on the immunostimulation of CpG-motifs on the DNA origami nanoparticles. When the adjacent CpG distance was positioned to be 7 nm, which matched the active dimer structure of the receptor, a high immunostimulatory property could be achieved (Fig. 3C).<sup>83</sup> More recently, Bathe's group investigated the immune activation of 3D wireframe DNA origami covered with CpG. When displaying multivalent CpG-containing ssDNA oligos, the wireframe DNA origami functionalized with multivalent CpG ODNs induced a robust immune response as evidenced by enhancements in the production of type I and type III IFNs. The CpG spatial organization and number each contributed to the TLR9 signaling magnitude.<sup>84</sup>

#### 2.5. DNA particles based on rolling circle amplification

In addition to DNA hybridization-induced nanostructures, the immune-stimulating capability of DNA particles based on rolling circle amplification was also investigated. Through an enzymatic rolling circle amplification method specifically based on a template encoded with the CpG sequence, the self-assembled DNA nanomedicine is composed of long-chain single-stranded DNA repeatedly containing interval CpG sequences. Tan and coworkers developed self-assembled immuno-nanoflowers consisting of long DNA integrated with tandem CpG *via* rolling circle amplification. The CpG-nanoflowers were demonstrated as potent immunostimulators by inducing immune cell proliferation, which subsequently secreted immunostimulatory cytokines such as TNF- $\alpha$ , IL-6 and IL-10. In addition, the therapeutic capability of CpG-nanoflowers to trigger cancer cell necrosis and apoptosis has been

efficiently proved.<sup>85</sup> Similar vaccines were conducted by producing tandem CpG and short hairpin RNA *via* rolling circle replication and transcription, which were subsequently loaded with tumor neoantigens. The microflower-shaped vaccine could significantly inhibit neoantigen-specific colorectal cancer *via* elicitation of CD8<sup>+</sup> T cell proliferation for effective cancer immunotherapy (Fig. 3D).<sup>86</sup> Gu's group also prepared the novel CpG ODN-based DNA nanococoon through rolling circle replication based on the CpG sequence-encoded template.<sup>87</sup> The CpG-based DNA nanococoon not only acted as the therapeutic loading matrix for anti-programmed cell death protein 1 antibody, but also can improve the anticancer immune response after fragmentation. More recently, Zhang and coworkers developed a photocontrolled DNA nanomedicine prepared by rolling circle amplification for the localized delivery of CpG and photosensitizer (TMPyP4) to enhance photodynamic immunotherapy. By blocking with a pH-triggered membrane-targeted peptide-modified cDNA, the DNA nanomedicine could be specifically anchored to the cancer cell membrane. The photodynamically triggered reactive oxygen species caused the breakage of DNA sequences after localized irradiation, which induced nanostructure collapses and internal DNA immunomodulator release for efficient antitumor treatment.<sup>88</sup>

#### 2.6. DNA hydrogel

Nishikawa and colleagues conducted a series of in-depth research studies on DNA hydrogel-based CpG and antigen delivery. X-shaped DNA containing six potent CpG motifs was devised as the building blocks for DNA hydrogel construction. The CpG DNA hydrogels were effective in terms of the TNF- $\alpha$  production by RAW264.7 cells, the dendritic cell maturation, and the delivery of doxorubicin to cancer cells, which exhibited efficient tumor inhibition capability.<sup>89</sup> In addition, the polypod-like structured DNA hexapodna could be further utilized as building units of injectable and self-gelling DNA hydrogel for both CpG and antigen delivery.<sup>90</sup> Sustained release of antigen ovalbumin could also be achieved through the intratumoral injection of DNA hydrogels containing cationized ovalbumin.<sup>91</sup> Additionally, the cationic ovalbumin peptide antigen composed of the ovalbumin MHC class I epitope linked to octaarginine could also be complexed with the CpG ODN hydrogel for an efficient antigen-specific cancer immune response.<sup>92</sup> Recently, Nishikawa's group also loaded the cedar pollen antigen Cryj1 in immune CpG hydrogel by applying self-gelatinizable DNA technology. Cryj1 loaded in CpG DNA hydrogel showed sustained release, enhancing the Cryj1-specific IgG production while suppressing the immunoglobulin E antibody generation for efficient immunotherapy for allergic symptoms.<sup>93</sup>

DNA nanocarriers are one ideal candidate for CpG delivery as they are fully biodegradable and controllable in shape and size at a tailor-made level.<sup>94-96</sup> In addition, DNA nanocarriers are also able to internalize into cells without assistance from any transfection agent.<sup>97,98</sup> Despite exciting progress in DNA nanocarrier development for CpG delivery, the following

aspects are still waiting to be achieved: (1) the effects of the sizes and structures of the DNA nanocarriers need to be investigated to further enhance immunostimulatory activities; and (2) multifunctional DNA nanocarriers, which can serve as versatile nanomedical platforms for the simultaneous co-delivery of CpG and other therapeutic agents (*e.g.* antigens, cancer drugs, photosensitizers), need to be developed as they are important components of combination cancer therapy.

### 3. Inorganic nanoparticle-based CpG delivery

The recent development of nanotechnology has brought about various inorganic nanomaterials as delivery carriers for CpG ODNs. Inorganic NPs, as CpG vehicles, are considered to be a promising nanoplatform for their various advantages, such as prolonged circulation time, superior cellular uptake and sustained release. Over the past two decades, multiple works have revealed the promise of inorganic nanoparticles for CpG delivery.

#### 3.1. Metal nanoparticles

Gold nanoparticles (AuNPs) offer a number of attractive features for drug delivery<sup>99,100</sup> because they are well known to be inert, biocompatible, and minimally immunoactive.<sup>101–103</sup> Thiol-modified CpG ODNs can be functionalized on AuNPs to form self-assembled CpG–AuNP nanoconjugates,<sup>104</sup> which were characterized by higher expressions of proinflammatory cytokines.<sup>105</sup> A drawback of the aforementioned method is that it requires thiolated CpG ODNs for AuNP conjugation. To simplify the synthesis procedure and achieve cost-effective drug delivery, a new approach for the facile synthesis of AuNP–CpG has also been developed.<sup>106</sup> It was found that the CpG motif with the poly-adenine (polyA) tail could easily be conjugated on the AuNPs' surface with tunable densities. The nanoassemblies were able to be efficiently taken up by RAW264.7 cells and induced an immune response. The polyA–CpG–AuNPs showed a much higher immune response than the thiolated counterparts under optimal conditions. In addition to gold nanoparticles, hollow gold nanospheres were also proved to be efficient nanocarriers for CpG delivery, resulting in higher immune stimulatory activity compared with CpG alone.<sup>107</sup> More recently, the effects of the sizes of gold nanoparticles on the immunostimulatory activity of CpG were also systematically investigated. The results indicated that size was the key factor in tuning the immunostimulatory activity of CpG–nanoparticles. The small 13 nm gold nanospheres showed a greatly higher specificity for targeting immune receptors, and larger 50 nm gold nanospheres and 40 nm gold nanostars displayed higher cellular uptake efficiencies and a stronger immune response owing to the off-target effects.<sup>108</sup> Furthermore, the nanostructure effects of gold nanoparticles on the CpG immunostimulatory activity were also explored. It has been revealed that different nanoconstructs composed of spiky or spherical gold nanoparticles conjugated with CpG had different endo-

somal distributions due to the distinct surface curvatures. The results indicated that, as compared with the spherical gold nanoparticles, the spiky gold nanoparticles with mixed-curvature constructs led to a higher percentage of hollow endosomes and a higher immunostimulatory activity.<sup>109</sup> Odom's group also studied how the endosomal pathways are influenced by their delivery order by sequentially incubating CpG-linked spherical and spiky gold nanoparticles with macrophages. Macrophages with a higher ratio of spiky to spherical nanoparticles at the endosomal edge, as well as a larger proportion of the enclosed spherical nanoparticles, displayed improved proinflammatory cytokine secretion.<sup>110</sup>

Previous studies have indicated that CpG ODNs and antigens should be co-localized in the same APCs to induce the most potent immune responses.<sup>111–113</sup> Therefore, the co-delivery of antigen and CpG ODNs on a single platform shows great potential to generate long-lasting and high immunity.<sup>77,114</sup> Advances in nanomaterials science have made it possible to deliver antigens and adjuvants with one single platform. Lee *et al.* suggested that the AuNPs could conjugate with both the model antigen red fluorescent proteins and the TLR9 ligand CpG ODNs to serve as the vaccine for effective cancer therapy.<sup>115</sup> Apart from utilizing the AuNPs as the CpG and antigen delivery platform, Tao *et al.* for the first time proved that CpG could be covalently linked to the antigen protein ovalbumin, which was applied as the template to synthesize gold nanoclusters (AuNCs) (Fig. 4A). The as-prepared AuNCs could simultaneously act as smart self-vaccines to help activate specific immunological responses through the co-delivery of CpG and protein antigens.<sup>116</sup>

In a similar approach, a facile one-pot method to synthesize fluorescent AuNCs through the peptide biomineralization strategy, which could elicit strong immune stimulatory ability, was also reported. As compared with that of the peptide alone, the immunostimulatory activity of the peptide-protected AuNCs was efficaciously improved. Furthermore, the peptide–AuNC–CpG conjugates were also able to serve as probes for intracellular trafficking as well as smart self-vaccines that can help induce high immunostimulatory activity. *In vitro* and *in vivo* results provided powerful evidence that the AuNC-based vaccines could be used as efficient and safe immunostimulatory agents for effective immunotherapy *via* the co-delivery of CpG and antigen peptides.<sup>117</sup>

The photothermal effects of gold nanomaterials could also be introduced to the Au–CpG nanosystem for combination hyperthermia and immune therapy. An interesting example of a multifunctional platform that showed multiple functions of hyperthermia, chemotherapy, and in particular immunotherapy, which could collaboratively contribute to efficient cancer therapy, was reported by Tao *et al.* The gold nanorods were conjugated with doxorubicin and CpG for cancer therapy. The introduction of AuNRs provided multiple merits, including high biocompatibility, great potential for hyperthermal therapy, as well as excellent carrying ability for anticancer agents and immunostimulatory signals. The Y-shaped CpG was effective at generating proinflammatory cytokines in

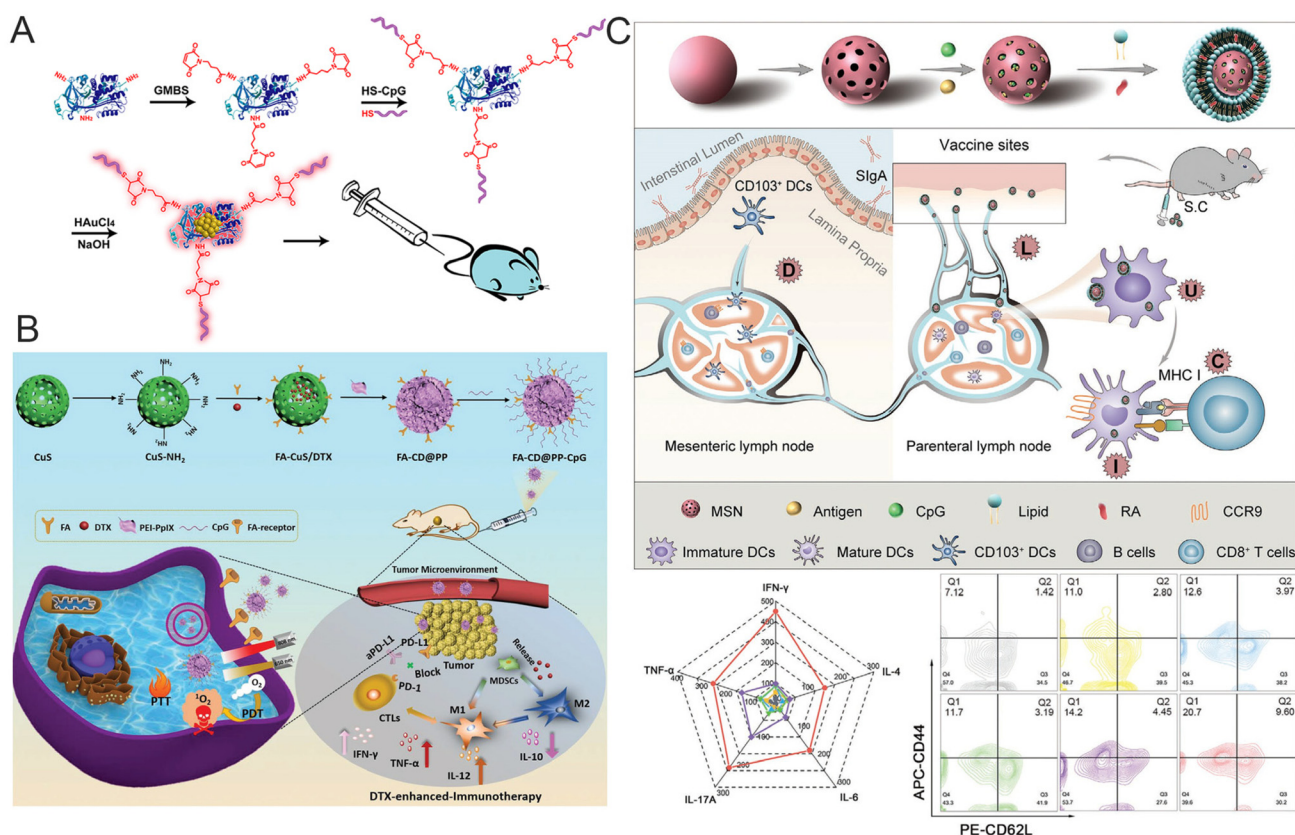


**Fig. 4** (A) General scheme for the synthesis of ovalbumin–AuNCs–CpG conjugates aimed at inducing an immune response.<sup>116</sup> Copyright 2014, Wiley-VCH. (B) Rational design and synthesis of folic acid–CuS/docetaxel@PEI/PpIX–CpG nanocomposites, their application in cancer treatment, and illustration of FA–CD@PP–CpG for docetaxel-enhanced immunotherapy.<sup>133</sup> Copyright 2019, Wiley-VCH. (C) Schematic illustration of the subcutis-to-intestine cascade for navigating mesoporous silica nanoparticles/lipid nanovaccines to simultaneously activate both cellular and mucosal immune responses. Accompanying this schematic is a contour map showing the levels of various cytokines collected from the supernatant of re-stimulated splenocytes, along with representative flow cytometric plots and the percentage of CD44<sup>+</sup>CD62L<sup>+</sup> T cells among CD8<sup>+</sup> T cells.<sup>159</sup> Copyright 2022, Wiley-VCH.

macrophage cells. This engineered nanovehicle showed significant antitumor efficiency.<sup>118</sup> Li and coworkers also developed a photothermal CpG nanotherapeutic, which integrated CpG ODNs with gold nanorods and assembled them with ovalbumin proteins, to suppress tumors *via* enhanced immunoefficiency. The photothermal gold nanorods induced a fever-like temperature of 43 °C, which could trigger an immunofavorable tumor microenvironment after intratumoral injection. High-throughput gene profile analysis identified the pyrogenic cytokine IL-6 upregulation.<sup>119</sup> Similarly, Qian's group also developed CpG@gold nanorods/polymer micelle encapsulated resiquimod (m-R848), for the combination photothermal and immunotherapy of melanoma. CpG@gold nanorods/m-R848 induced great antitumor effects by reprogramming of M2 macrophages into the M1 phenotype and promoting the maturation of dendritic cells. Furthermore, immunogenic cell death triggered by the photothermal ablation of gold nanorods could synergistically generate lasting and systemic antitumor immunity.<sup>120</sup> Recently, *in situ* photothermal nanovaccines were also constructed by encapsulating indoleamine 2,3-dioxygenase inhibitors together with CpG-loaded black phosphorus-

gold nanosheets by a cancer cell membrane, for effective primary and metastatic breast cancer therapy.<sup>121</sup> Park and colleagues prepared novel multifunctional nanoadjuvants composed of cationic polymer shells and iron oxide/gold cores with CpG complexed on the surfaces through electrostatic interactions. The nanoadjuvants could be retained for a prolonged time in the tumoral extracellular matrix and internalized into antigen-presenting cells after intratumoral injection. The irreversible electroporation could trigger immunogenic cell death. The combination therapy resulted in great tumor inhibition with a 100% survival rate for about 60 days.<sup>122</sup> On the other hand, gold nanorods–CpG-based nanomedicines for radio-immunotherapy were also developed. The first procedure of the two-step low-dose radiotherapy strategy was engaged to recruit plenty of macrophages into the tumor to switch M2 macrophages to M1 phenotypes. The nanomedicine in the tumor sensitized the second dose of radiotherapy, leading to a synergistic treatment of cancer.<sup>123</sup>

The current progress in nanomedicine also involves the combination of imaging and therapeutic functions. An easy method for preparing CpG-functionalized silver nanoclusters



(CpG–AgNCs), integrating attractive characteristics of imaging and improved immune response, has been reported.<sup>124</sup> The AgNCs provided several crucial merits including improved CpG uptake by TLR9-positive cells, and enhanced CpG stability against nuclease degradation, which were extremely important for enhancing the immunostimulatory activity of CpG–AgNCs. In addition, the CpG–AgNCs with compelling fluorescence features could simultaneously serve as optical nanoprobe for bioimaging. Similarly, for the first time, Tao *et al.* also devised the facile one-step synthesis of CpG-functionalized CdTe quantum dots that combined fascinating characteristics of cell imaging and enhanced immunogenicity.<sup>125</sup> Furthermore, Ming *et al.* employed palladium nanosheets as carriers to load the immunoadjuvant CpG, which could be effectively applied to combinatorial cancer photothermal and immunotherapy both *in vitro* and *in vivo*.<sup>126</sup> Recently, Chen and coworkers proposed an efficient anticancer strategy with integrated chemodynamic/photodynamic/photothermal modalities by *in situ* constructing black phosphorous/palladium nanosheets. The immune adjuvant CpG could be efficiently loaded onto the nanosheets after fluoropolyethyleneimine modification, further improving tumor therapeutic efficacy.<sup>127</sup>

### 3.2. Metal oxide and sulfide nanomaterials for CpG delivery

Metal oxide and metal sulfide nanomaterials are novel classes of metal-containing nanomaterials composed of metal ions and oxygen or sulfur compounds. During the past decade, scientists found that the metal oxide and sulfide nanomaterials engineered by specific approaches not only had high biocompatibility but also exhibited unique physicochemical properties for CpG delivery, such as a large surface area, high drug loading ability and metal-enhanced immunostimulatory activities. Qu and colleagues developed a MnO<sub>2</sub>–CpG–AgNCs–doxorubicin nanoconjugate for efficient cancer immunotherapy, in which the support MnO<sub>2</sub> nanosheets could integrate CpG–AgNCs and doxorubicin *via*  $\pi$ – $\pi$  interactions for remarkable anticancer activity.<sup>128</sup> Similarly, He *et al.* also developed an immune nanoplateform composed of CpG and MnO<sub>2</sub> within nanogels consisting of poly(*N*-vinylcaprolactam) for immunoadjuvant, magnetic resonance imaging-guided radiotherapy against glioblastoma multiforme.<sup>129</sup> Recently, Park and colleagues developed metal–phenolic network-based immunostimulating nanoplateforms, which were synthesized by coordinating Mn ions with tannic acid, and subsequently coating them with CpG. The nanoparticles successfully triggered the M1 polarization of macrophages to promote proinflammatory cytokine release, leading to tumor inhibition.<sup>130</sup> More recently, Mn<sup>2+</sup> was also reported to promote the production of type I interferons, thus improving the infiltration of cytotoxic T lymphocytes, the maturation of dendritic cells, and the secretion of proinflammatory cytokines.<sup>131</sup>

In addition to Mn-based nanocarriers, Lu's group reported on the design of chitosan-decorated hollow CuS NPs loaded with CpG motifs as an NIR-induced transformative nanoplateform. The laser could induce the breakdown of CuS NPs, improving the tumor retention. The photothermal ablation

triggered the release of the tumor antigens, while the CpG potentiated host antitumor immunity, resulting in the effective treatment of primary and distant tumors.<sup>132</sup> Dong's group constructed folic acid-modified, docetaxel-loaded, polyethyleneimine–protoporphyrin IX and CpG conjugated mesoporous CuS nanoparticles as a multifunctional nanoplateform for cancer synergistic phototherapy and immunotherapy. The nanocomposites could induce significant damage to tumors when combined with anti-PD-L1 antibodies for immunotherapy and laser irradiation for photodynamic and photothermal therapy. The docetaxel in the nanocomposites could enhance the cytotoxic T lymphocyte infiltrations, and effectively polarize myeloid-derived suppressor cells to promote proinflammatory cytokine generation, thus leading to reinforced antitumor efficacy (Fig. 4B).<sup>133</sup> Similarly, MoS<sub>2</sub> nanosheets–poly(ethylene glycol) (PEG)–CpG was also fabricated as the multifunctional nanoplateform for photothermal enhanced immunotherapy. The MoS<sub>2</sub>–PEG–CpG nanoconjugates with excellent triggered effects could significantly elevate CpG intracellular accumulation and remarkably promote the immune responses, which dramatically reduced the proliferative activity of tumor cells.<sup>134</sup>

### 3.3. Calcium-based biomineralized nanomaterials for CpG delivery

Calcium phosphates with excellent biocompatibility and biodegradability are the main inorganic constituents of biological hard tissues such as teeth and bones, and therefore they are promising as excellent bioabsorbable biomaterials for a broad range of biomedical applications, such as medical treatment, diagnosis, and tissue engineering.<sup>135,136</sup> Calcium phosphate is also capable of delivering both antigen and CpG delivery. In the nanoparticulate form, it can be easily taken up by the cells and then dissolved in the lysosomes.<sup>137</sup> Inspired by these advantages, Westendorf and Epple developed calcium phosphate NPs that could carry immunoactive oligonucleotides and antigens for DC activation.<sup>112</sup> After that, the same group also prepared calcium phosphate NPs as carriers for the viral antigen hemagglutinin combined with polyinosinic–polycytidylic acid and CpG for the activation of DCs. Studies indicated that purified calcium phosphate NPs were capable of triggering adaptive immunity *via* cytokine secretions and elevated co-stimulatory molecules and MHC II expression.<sup>138</sup> In another instance, lipid–calcium–phosphate NPs modified with mannose as the vaccines to deliver the adjuvant CpG and tumor antigen Trp 2 peptide were developed.<sup>139</sup> In addition, targeted silencing of immune-suppressive cytokine expressions of TGF- $\beta$  in the tumor microenvironment with liposome–protamine–hyaluronic acid NPs further improved the vaccine efficacy in an advanced melanoma model. Arami and coworkers also synthesized calcium phosphate NPs applying various CpG types as templates for mineralization for improved immunostimulatory effects. The effects of sequences, backbones, and concentrations of the CpGs on the formation of calcium phosphate nanoparticles were evaluated. The mineralization of calcium phosphate was blocked at increased phosphodiester concentrations, but this effect was

not observed for the phosphorothioate groups more than a certain range.<sup>140</sup>

### 3.4. Carbon nanomaterials for CpG delivery

Carbon materials have attracted wide attention in biomedical applications owing to their large surface area, photothermal properties, chemical stability and low cost.<sup>141</sup> The applications of carbon materials have also been extended to immunotherapy in recent years. Since their serendipitous discovery in 1991, carbon nanotubes (CNTs) have attracted significant interest from the scientific communities due to their unique physical and chemical properties.<sup>142</sup> CNTs, as novel drug delivery vehicles, have also been widely used for CpG delivery. In 2004, Partidos and Prato found that cationic ammonium-functionalized CNTs were advantageous for effective CpG delivery into target cells, increasing the immunostimulatory properties of linked CpG ODNs.<sup>143</sup> CNTs have also shown promise for the cancer-testis antigen NY-ESO-1 and adjuvant CpG delivery.<sup>144</sup> The CNT nanoconstructs induced strong CD8<sup>+</sup> and CD4<sup>+</sup> T-cell-mediated immune activities against NY-ESO-1, which significantly prolonged mouse survival and delayed tumor development.

Graphene oxide (GO) exfoliated from oxidized graphite is generally considered to be the candidate material for biomedical applications because of its excellent aqueous processability and ultrahigh drug loading efficiency.<sup>145</sup> The ability of GO to act as a CpG nanocarrier was explored. Immunostimulatory CpG ODNs could be loaded onto poly(L-lysine)-modified uniform small or polydisperse GO nanosheets. The uniform small GO-CpG appeared to be the more efficient stimulator in stimulating immunostimulatory activity as compared with polydisperse GO-CpG nanosheets. Recently, graphene has also been extensively investigated for biomedicine applications due to its drug-carrier and photothermal properties.<sup>146,147</sup> Inspired by these investigations, Tao *et al.* applied GO modified with PEG and PEI for the efficient delivery of CpG ODNs (GO-PEG-PEI-CpG). A photothermally induced, remarkably improved immunogenicity of GO-PEG-PEI after NIR irradiation could be observed, which could be attributed to the accelerated intracellular trafficking of nanovectors. The synergistic immunological and photothermal effects of the GO-PEG-PEI-CpG induced excellent efficiency in cancer therapy.<sup>148</sup> Liu and coworkers fabricated CpG ODN and NIR photosensitizer IR820 dual-dressed and triphenylphosphonium-functionalized nanographene for mitochondria-targeted cancer immunotherapy, photothermal therapy and photodynamic therapy. The IR820 generated photothermal heat and abundant ROS to kill cancer cells, while the CpG remarkably enhanced the immunostimulatory activities. *In vivo* research proved that the nanographene hybrid significantly inhibited tumor growth and caused negligible toxic effects on mice.<sup>149</sup>

### 3.5. Silica nanomaterial-mediated CpG delivery

Silica nanomaterials are typical inorganic nanomaterials that possess many advantages including low cost, easy scale-up,

convenient surface functionalization, a hydrophilic nature and excellent biocompatibility.<sup>150,151</sup> Over the last ten years, one of the hottest areas in nanobiotechnology and nanomedicine has been the design of biocompatible silica nanomaterials and multifunctional counterparts in disease theranostics.<sup>152</sup> Hanagata and Chen synthesized silica nanotubes with tailored lengths, which could be linked with chitosan for immunostimulatory CpG delivery.<sup>153</sup> The decreased length of the silica nanotubes led to greater CpG cellular uptake and an enhanced immunostimulatory response, suggesting the potential application in immunotherapy. Another example showed that PEG-modified, amine magnetic mesoporous silica NPs could also be utilized as CpG delivery nanovectors. The PEG-conjugated magnetic mesoporous silica NPs showed negligible cytotoxicity, excellent CpG loading capacity, and the ability to be easily internalized into cells. These nanocomplexes combined with chemotherapeutics could greatly kill the tumor cells *via* activating macrophages.<sup>154</sup> Similarly, the triethoxypropyl-aminosilane functionalized silica nanoparticles could also be utilized as effective nanocarriers for the targeted transportation of ovalbumin antigens and CpG adjuvants to draining lymph nodes, driving a notable antitumor immune response with high safety.<sup>155</sup> Wang's group developed a cancer vaccine by using mesoporous silicon vectors for the co-delivery of tyrosinase-related protein 2 peptide and two different TLR agonists (monophosphoryl lipid A and CpG), increasing the capacity of dendritic cells to induce potent tyrosinase-related protein 2-specific CD8<sup>+</sup> T cell responses for highly efficient tumor immunotherapy.<sup>156</sup> Yantasee and coworkers also designed biodegradable mesoporous silica nanoparticles to co-deliver STAT3 siRNA and CpG to induce efficient whole-body antitumor immunity. In combination with systemic immune checkpoint inhibitors, the immunotherapy based on the silica nanoparticle co-delivery of STAT3 siRNA and CpG completely cured 63% of mice with melanoma tumors.<sup>157</sup> Recently, Li *et al.* developed lipid-coated mesoporous silica nanoparticles for CpG and TLR7/8 agonist resiquimod (R848) delivery. The nanoplatform could greatly improve the antitumor efficacy *via* remarkably modulating the tumor immunosuppressive microenvironment by repolarizing macrophages from the M2 to M1 phenotype, facilitating the maturation of dendritic cells, and promoting the infiltration of tumor cytotoxic T cells.<sup>158</sup> Similarly, Zhong *et al.* also encapsulated mesoporous silica nanoparticles with adjuvant CpG and antigen, and further coated them with an all-*trans* retinoic acid contained lipid bilayer. The mice dramatically generate protective immune responses against *S. typhimurium* challenge after being vaccinated with *Salmonella enterica* serovar Typhimurium antigen-loaded nanovaccine (Fig. 4C).<sup>159</sup>

## 4. Polymeric nanocarriers for CpG delivery

Polymeric materials have attracted wide interest owing to their broad applications in diverse fields, including diagnostics, and

therapeutics, smart coatings and textiles, as well as tissue engineering.<sup>160</sup> One of the foremost fields among these applications is developing optimized polymer nanoparticle-based delivery systems, due to their great promise as carriers for chemotherapeutics, nucleic acid, peptides and proteins with high loading capacities.<sup>161</sup> Therefore, CpG ODNs can also be efficiently delivered and protected against nuclease degradation by polymer NPs.

#### 4.1. Natural polymer-based particles/nanocomposites for CpG delivery

**4.1.1. Chitosan.** As one of the most widely used polymers, chitosan NPs can be utilized to efficiently deliver CpG ODNs. Chitosan/CpG ODN NPs could be synthesized by using the novel microfluidic technique or the conventional bulk mixing method. The microfluidic-processed NPs exhibited much stronger immunity as compared with mixing-processed NPs.<sup>162</sup> Leong and coworkers developed nanovaccines *via* polyelectrolyte complexation of heparin and chitosan to encapsulate the VP1 protein antigen with CpG or TNF- $\alpha$  as adjuvant. The nanovaccines showed prolonged retention in lymph nodes and induced great Th1 and Th2 immune activations, conferring effective protection against lethal virus challenges. Moreover, the nanovaccines could also elicit high IgA titers, which might provide great advantages for mucosal protection.<sup>163</sup> Moreover, a self-degradable conjugated polyelectrolyte to load CpG for the combination of photodynamic therapy-induced immunogenic cell death and immunotherapy of CpG was also developed for systemic antitumor immunity.<sup>164</sup>

**4.1.2. Hyaluronic acid.** Hyaluronic acid is a natural polysaccharide with good biocompatibility and degradability. Hyaluronic acid and its derivatives can be used as sustained-release carriers for CpG, which can delay the release of CpG and have a long-acting effect. Kim's group highlighted the importance of multivalency in enhancing the immunostimulatory activity of CpG. They synthesized hyaluronic acid-based multivalent nanoconjugates, augmenting immunostimulation by combining these with CpG ODNs and cationic poly(L-lysine), a widely used transfection agent. The resultant hyaluronic acid-CpG nanoconjugate efficiently activated the antigen-presenting cells, while the poly(L-lysine)/hyaluronic acid-CpG nanocomplex improved cellular uptake and sustained endosomal TLR9 stimulation. Vaccination of mice with dendritic cells treated with this nanocomplex inhibited tumor growth and elicited robust antitumor memory responses.<sup>165</sup> Li *et al.* developed a polydopamine-coated, hyaluronic acid-shelled nanoparticle loaded with CpG ODNs, which induced strong antitumor immune responses and photothermal ablation. The CpG ODNs effectively matured dendritic cells by upregulating co-stimulatory markers. Their approach synergistically combined photothermal therapy with CpG ODNs, demonstrating significant treatment efficacy in a melanoma-bearing mouse model.<sup>166</sup> Chen's group innovated a hyaluronic acid/PEI-KT-based delivery system to co-deliver OX40L plasmids and CpG. This strategy facilitated the expression of OX40 on T cells within tumors, and the anchoring of OX40L on tumor cell

membranes, thus enhancing T cell responses. This approach effectively transformed "cold" tumors into "hot" ones, sensitizing them to PD-1/PD-L1 blockade therapy and preventing tumor recurrence and metastasis in both 4T1 and B16F10 tumor models (Fig. 5A).<sup>167</sup> Malfanti and colleagues designed bioresponsive hyaluronic acid-doxorubicin/CpG conjugates for the *in situ* chemoimmunotherapy of glioblastoma. They combined CpG, a TLR-9 agonist, with doxorubicin, an immunogenic cell death inducer, to synergistically eradicate tumors. The local administration activated antitumor CD8<sup>+</sup> T cell responses, reduced myeloid-derived suppressor cells and M2-like tumor-associated macrophage infiltration in the brain tumor microenvironment, and significantly extended the survival of glioblastoma-bearing mice.<sup>168</sup>

**4.1.3. Gelatin.** Gelatin, derived from collagen, is biocompatible and amendable to modification for crosslinking with visible light.<sup>169</sup> In 2008, Zwiorek *et al.* utilized cationized gelatin nanoparticles as biodegradable carriers to enhance the immunostimulatory CpG delivery. The use of these cationized gelatin nanoparticles for delivering class-B and class-C CpG ODNs to primary human plasmacytoid dendritic cells resulted in increased production of IFN- $\alpha$ , a crucial cytokine for the activation of both innate and adaptive immunity.<sup>170</sup> Similarly, Neek *et al.* explored the immune responses elicited by nanoparticle formulations of the E2 subunit assembly of pyruvate dehydrogenase, incorporating cancer-testis antigens MAGE-A3 and NY-ESO-1, along with the CpG adjuvant. Their *in vivo* studies demonstrated that immunization with these vaccine nanoparticles not only significantly increased IFN- $\gamma$  expression but also enhanced lysis activity against target A375 cells.<sup>171</sup>

#### 4.2. Synthetic polymer-based nanoparticles for CpG delivery

**4.2.1. Poly(lactic-co-glycolic acid) (PLGA).** Poly(lactic-co-glycolic acid) (PLGA), an FDA-approved biocompatible and biodegradable polymer, is extensively researched for drug delivery due to its advantageous properties.<sup>172,173</sup> PLGA has been particularly utilized for transporting antigens and CpG ODNs. An early application by Diwan's group involved co-delivering CpG ODN and antigens in biodegradable PLGA nanoparticles, using tetanus toxoid as a model antigen. Their findings showed that T cells from mice immunized with this formulation exhibited higher IFN- $\gamma$  secretion and enhanced antigen-specific proliferation compared with reference groups.<sup>174</sup> More recently, manipulated PLGA has been used for CpG delivery, combined with glioma homing peptide-modified paclitaxel targeting nanoparticles, for the chemo-immunotherapy of glioma *via* local delivery in the resection cavity.<sup>175</sup>

The development of pathogen-mimicking PLGA nanoparticles through facile dopamine polymerization has shown great promise as vaccine and adjuvant delivery systems. These functionalized nanoparticles can enhance cytokine secretion, and immune cell recruitment, activate and mature DCs, and induce robust humoral and cellular immunity.<sup>176</sup> Similarly, Pradhan's group developed synthetic PLGA particulate nanocarriers co-loaded with CpG and monophosphoryl lipid A. These pathogen-like particles elicited synergistic interleu-

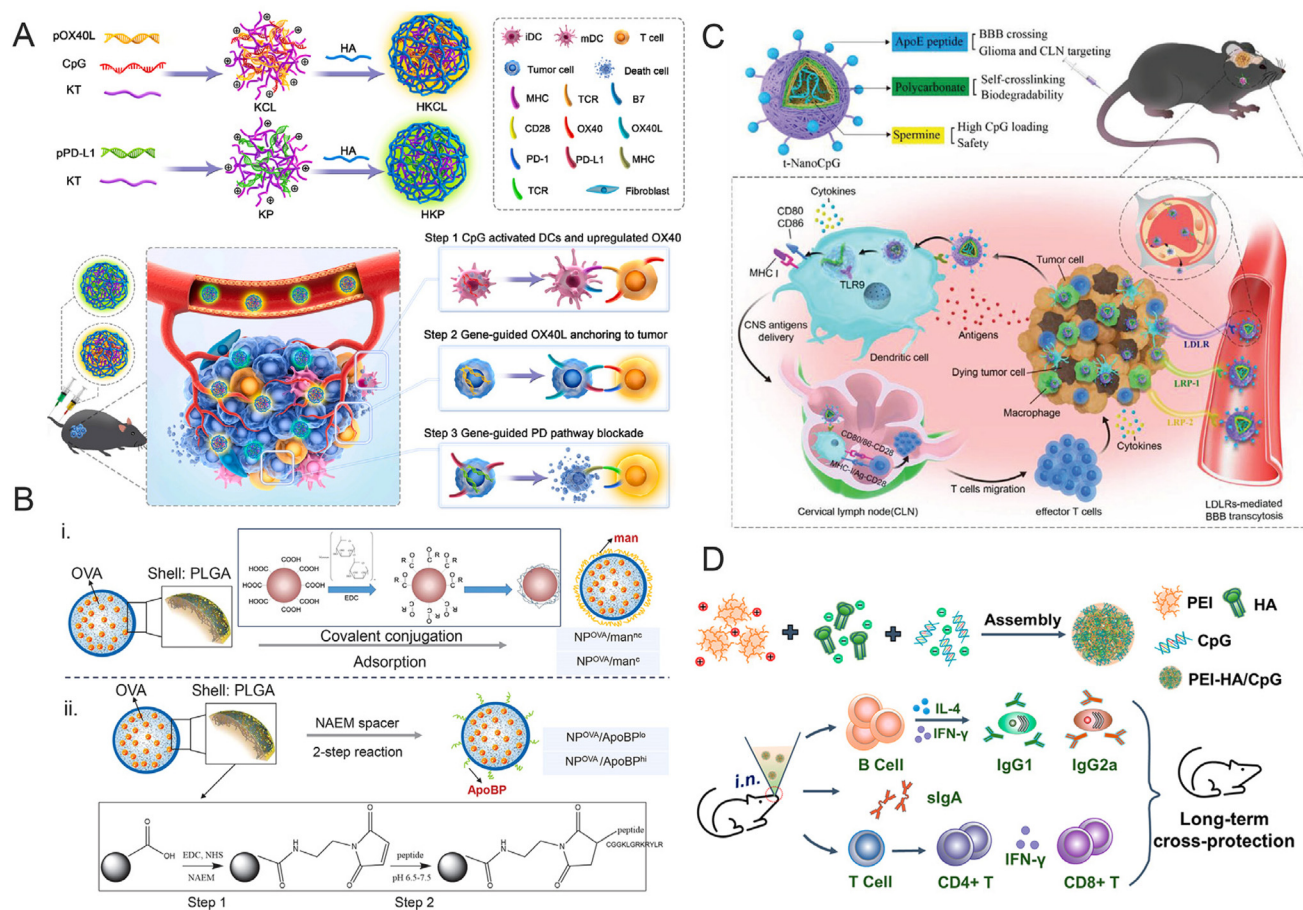


**Fig. 5** (A) Schematic illustration of anchoring OX40L to tumor cell membrane for synergistic tumor "self-killing" immunotherapy.<sup>167</sup> Copyright 2023, Elsevier. (B) Synthesis of the liver sinusoidal endothelial cell-targeting PLGA NP platform for ovalbumin delivery. Schematic showing particle surface decoration with mannan and ApoBP.<sup>180</sup> Copyright 2019, American Chemical Society. (C) Schematic of apolipoprotein E peptide-functionalized polymersome CpG nanoformulation structure and strategy for enhancing the intracellular delivery of CpG in orthotopic glioma and cervical lymph nodes.<sup>188</sup> Copyright 2022, Wiley-VCH. (D) Schematic illustration of the PEI-HA/CpG nanoparticle preparation and the induced immune responses.<sup>190</sup> Copyright 2022, American Chemical Society.

kin-12p70 and interferon- $\beta$  responses in granulocyte-macrophage colony-stimulating factor-driven mouse bone marrow-derived antigen-presenting cells.<sup>177</sup> Du *et al.* employed mannosylated PLGA/PLAG-PEG Pickering emulsions with unique hierarchical structures to target antigen-presenting cells. These emulsions synergistically delivered CpG and antigenic peptides, increasing the droplet-cell contact area and enhancing the cellular recognition of mannanose and CpG for improved immune activation. When combined with PD-1 antibodies, this nanovaccine significantly regressed tumors, showing a synergistic enhancement in anti-tumor effects.<sup>178</sup>

CpG-based immunotherapy has been effectively integrated with other therapeutic methods, utilizing PLGA nanoparticles as optimal platforms for the co-delivery of multiple therapeutic agents. Groettrup *et al.* developed biodegradable PLGA microspheres for delivering antigens and TLR ligands to APCs. These PLGA microspheres, encapsulating model antigens, efficiently presented these antigens on MHC class I and II molecules of DCs, thereby stimulating robust cytotoxic and T

helper cell responses.<sup>179</sup> In addition, they also utilized PLGA microspheres encapsulating both CpG and tumor lysates, as well as polyI:C, to provoke antitumor activities. Moreover, the biodegradable PLGA nanocarrier was also applied in delivering the murine allergen ovalbumin to the liver. These nanoparticles were tailored with ligands targeting mannose receptors and scavengers on liver sinusoidal endothelial cells. Prophylactic treatment using these ovalbumin-loaded nanoparticles in sensitized and challenged animals greatly reduced TH2 cytokine production, anti-ovalbumin IgE responses, and airway eosinophilia in bronchoalveolar lavage fluid. The addition of ApoB peptides as a surface ligand further amplified the inhibitory effect, underscoring the potential of ovalbumin-loaded PLGA nanocomposites in the treatment of allergic airway diseases (Fig. 5B).<sup>180</sup>

**4.2.2. Poly(propylene sulfide) (PPS).** Poly(propylene sulfide) (PPS) nanoparticles are considered effective for CpG and antigen delivery, owing to their ultrasmall size that facilitates efficient drainage to the lymph nodes and targets a sig-

nificant proportion of resident DCs. For instance, a Pluronic-stabilized PPS NP-based nanocarrier for CpG and ovalbumin delivery was designed to specifically target pulmonary DCs upon delivery to the lungs, enhancing antigen transport to the draining lymph nodes. Pulmonary immunization with NP-conjugated CpG and ovalbumin resulted in a threefold enhancement in splenic antigen-specific CD8<sup>+</sup> T-cell immunity, exhibiting increased IFN- $\gamma$  expression compared with immunization with unconjugated CpG and ovalbumin.<sup>181</sup> Additionally, the ability of adjuvants CpG-B or CpG-C with a low adjuvant dosage to target lymph nodes using ultrasmall polymeric PPS NPs has been explored. These NPs could rapidly be drained to the lymph node after intradermal injection, leading to improved Th1-cytokine secretion and dendritic cell maturation, resulting in stronger effector CD8<sup>+</sup> T-cell activation with more robust memory recall. Notably, NP-CpG-B provided substantial protection against syngeneic tumor challenges even four months post-vaccination. These findings collectively demonstrate that nanocarriers can significantly increase vaccine efficacy, resulting in long-lasting cellular immunity.<sup>182</sup>

**4.2.3. Polypeptide.** DNA-loaded polypeptide particles for delivering adjuvant CpG ODNs were synthesized using mesoporous silica templating and a thiol-disulfide exchange cross-linking method. The cargo loading ability of these particles was adjustable based on the amount of cross-linker used, enhancing their stability. These polypeptide nanoparticles effectively delivered their cargo to primary human pDCs and activated them. *In vitro* experiments revealed that particles with higher loading capacities led to enhanced vaccine immunogenicity.<sup>183</sup> Chilkoti's group recently developed an injectable depot composed of thermally sensitive elastin-like polypeptides for CpG immunostimulant and iodine-131 radionuclide delivery. These polypeptides, featuring an oligolysine tail, formed an electrostatic complex with CpG for immunotherapy. When combined with iodine-131-elastin-like polypeptides for brachytherapy, the treatment notably inhibited 4T1 tumor growth and significantly reduced the development of lung metastases.<sup>184</sup> Additionally, a novel ApoE peptide-mediated systemic nanodelivery system was developed for co-delivering granzyme B and CpG. This system was designed to enhance the immunotherapy of a murine malignant glioma model, providing a promising approach for advanced cancer treatments.<sup>185</sup>

**4.2.4. Poly(ethylene glycol) (PEG).** PEG is the most used polymer and also the gold standard for stealth polymers in the emerging field of polymer-based drug delivery. PEG is non-toxic, highly soluble in water and FDA approved. The PEG-based delivery nanosystems have several advantages including a prolonged residence in body, and a decreased degradation by metabolic enzymes. Lv's group developed a PEG hydrogel for dual fluorescence imaging-tracked, programmed delivery of CpG nanoparticles and doxorubicin, aimed at modulating the tumor microenvironment for efficient chemo-immunotherapy.<sup>186</sup> The combined stimulation of CpG nanoparticles and doxorubicin positively altered the tumor microenvironment, evidenced by an increase in cytotoxic CD8<sup>+</sup> T lymphocytes and

a decrease in M2-like tumor-associated macrophages and myeloid-derived suppressor cells. This modulation heralded favorable therapeutic responses, offering a promising approach for advanced cancer therapy. Perry *et al.* employed PRINT (particle replication in nonwetting templates) nanoparticles, composed of PEG700 diacrylate, amino ethyl methacrylate, and hydroxyl-terminated PEG248 acrylate, to deliver CpG into murine lungs through orotracheal instillation. This approach extended CpG retention in the lungs and prolonged the elevation of antitumor cytokines, effectively inducing substantial tumor regression in lung cancer metastasis models.<sup>187</sup> Additionally, Zhong and colleagues synthesized a glioma and cervical lymph node-homing and blood-brain barrier permeable CpG nano-immunoadjuvant through the co-self-assembly of PEG-polycarbonate-spermine, apolipoprotein E peptide-PEG-polycarbonate, and CpG. Remarkably, both intranasal and intravenous administration of this targeting CpG nano-immunoadjuvant significantly improved survival in murine LCPN glioma-bearing mice (Fig. 5C).<sup>188</sup>

**4.2.5. Polyetherimide (PEI).** PEI has been widely studied for the design of nucleic acid delivery vehicles. PEI, being positively charged, is able to form nanoscale complexes with CpG ODNs, leading to CpG protection, cellular delivery, and intracellular release. Wang's group engineered a transcutaneous tumor vaccine delivery system by applying mannosylated PEI-modified ethosomes encapsulated in an electrospun nanofibrous patch. This system demonstrated efficient targeting of DCs. The mannosylated PEI-modified ethosomal carriers, loaded with tyrosinase-related protein-2 peptide antigen and adjuvant, effectively induced DC maturation, leading to an effective antitumor effect.<sup>189</sup> In another study, Wang and colleagues created PEI-hemagglutinin/CpG nanoparticles to explore their immune responses using an intranasal vaccination regimen in mice. These nanoparticles elicited more balanced and robust IgG1/IgG2a antibody responses with enhanced Fc-mediated antibody-dependent cellular cytotoxicity and neutralization activity. Additionally, the PEI-HA/CpG nanoparticles induced stronger systemic and local cellular immunity over a six-month observation period post-immunization, demonstrating the synergistic effect of PEI and CpG (Fig. 5D).<sup>190</sup> Mooney's group developed a cryogel vaccine system where the release of CpG could be induced on-demand using ultrasound. CpG was condensed with PEI and then adsorbed onto cryogels. Ultrasound stimulation 4 days post-vaccination significantly heightened the antigen-specific cytotoxic T-lymphocyte response. Moreover, this ultrasound stimulation also resulted in a notably high IgG2a/c antibody titer, underlining the potential of this approach for targeted vaccine delivery.<sup>191</sup>

**4.2.6. Copolymer-based nanoformulations.** Advances in polymer chemistry and polymerization methods offer the opportunity to synthesize copolymers with a variety of block combinations. Copolymers hold great potential for improving the effectiveness of therapeutic CpG molecules owing to the easy adjustability of their size, stability and surface chemistry. Lymph nodes, being critical targets of cancer vaccines, can be

effectively targeted by polymeric hybrid micelles with tunable particle sizes and surface charges, enhancing lymph node retention and antigen-presenting cell uptake. Li *et al.* developed polymeric hybrid micelles composed of two amphiphilic diblock copolymers: polycaprolactone–polyethylene glycol and polycaprolactone–polyethylenimine. These were used in varying proportions to efficiently load CpG and melanoma antigen peptide tyrosinase-related protein 2 for melanoma immunotherapy. The formulation containing 10% cationic polycaprolactone–polyethylenimine achieved an optimal balance, demonstrating effective lymph node distribution and a strong immune response.<sup>192</sup> Following this, the same group developed another type of polymeric hybrid micelle for encapsulating CpG and tyrosinase-related protein 2. These micelles self-assembled from cationic polyethylenimine–stearic acid conjugate and anionic poly-(ethylene glycol) phosphorethanolamine through electrostatic and hydrophobic interactions. The optimized ratios in this co-delivery system resulted in significant cytotoxic T lymphocyte activity, and reduced melanoma tumor growth and metastasis.<sup>193</sup> Ohya's group created hyaluronic acid-coated biodegradable poly(L-lysine)-*b*-polylactide micelles as nanoparticulate vaccine delivery systems. These efficiently loaded CpG and ovalbumin, facilitating the establishment of an effective nasal vaccine. The polymeric micelles upregulated mRNA encoding IL-4 and IFN- $\gamma$ , and enhanced the expression of ovalbumin-specific IgG levels in the blood.<sup>194</sup> Zhong's group synthesized cRGD-functionalized chimeric polymersomes for the efficient delivery of oncolytic peptide LTX-315. Combined with anti-PD-1 and CpG, this formulation boosted melanoma immunotherapy. Systemic administration led to notable tumor accumulation and significant tumor growth retardation. The treatment efficacy was further enhanced by co-administering anti-PD-1 antibody and polymersome CpG, resulting in complete cures in two out of seven mice due to the strong immunization effect and robust antitumor memory recall.<sup>195</sup>

## 5. Metal–organic-framework (MOF)-based CpG delivery systems

### 5.1. Zeolitic imidazolate framework-8 (ZIF-8) nanoparticles

Metal–organic frameworks (MOFs), comprising porous crystalline inorganic–organic hybrids of bridging metal ions or clusters coordinated to organic ligands,<sup>196,197</sup> have gained prominence across various fields due to their structural diversity, ultrahigh surface areas, customizable surface modifications, and tunable pore sizes. These properties have led to their widespread use in sensing, gas storage, catalysis, and small molecule separation.<sup>198–200</sup> Recently, MOFs have seen significant advancements in biological applications, particularly as drug delivery systems, and have been extensively explored for subunit vaccine development.<sup>201–203</sup> Zhang *et al.* were pioneers in this area, reporting the facile synthesis of nanoscale MOFs ZIF-8-based subunit vaccines.<sup>204</sup> These vaccines encapsulate protein antigen ovalbumin and absorb immune adjuvant CpG,

eliciting robust cellular and humoral immune responses. The resulting ovalbumin@ZIF-8–CpG vaccines showcased pH-responsive dissociation properties, enabling efficient CpG and antigen delivery to the same antigen-presenting cells. Both *in vitro* and *in vivo* experiments demonstrated that these vaccines could induce strong immunity and a high immune memory response.<sup>205</sup> Furthermore, leveraging the porous structure of ZIF-8 nanoparticles, Zhang *et al.* also developed a CpG nanocarrier nanosystem by loading CpG into ZIF-8. This approach enhanced intracellular CpG uptake and facilitated effective CpG release under acidic conditions, thereby increasing the immune cytokine secretions in both *in vitro* and *in vivo* settings.<sup>206,207</sup>

### 5.2. Zirconium UIO-66

UIO-66 as a rather ubiquitous MOF consists of zirconium ions that are surrounded by bonded terephthalic ligands. These components and structures make an active, spacious surface area with biodegradability alongside low cytotoxicity. Fan and colleagues developed CpG–MOF nanocomposites with a high density of CpG, utilizing multivalent coordination between the unsaturated zirconium sites on the UIO-66 and the phosphate backbone of CpG. These nanocomposites were further enhanced with a calcium phosphate exoskeleton protection shell. This shell not only provided DNA protection but also supplied high concentrations of phosphate ions for controlled CpG release. The calcium phosphate-coated CpG–MOF nanocomposites exhibited an 83-fold increase in cytokine secretion compared with uncoated CpG–MOF (Fig. 6A).<sup>208</sup> Additionally, zirconium-based nanoscale MOFs were found to not only facilitate CpG delivery, enhancing immunostimulatory activity, but could also be modified with DNA aptamers *via* coordination chemistry to target specific cancer cells.<sup>209</sup> Pang *et al.* functionalized CpG-loaded zirconium UIO-66 nanoparticles with bone-targeting zoledronic acid to address breast cancer-associated osteolysis. These bone-targeting MOF nanoparticles effectively inhibited osteoclast formation and simultaneously induced macrophage polarization to the M1 phenotype.<sup>210</sup> Furthermore, multifunctional MOF nanosystems were fabricated by self-assembling zirconium ions with a photosensitizer (tetrakis(4-carboxyphenyl)porphyrin). These systems combined photodynamic therapy with acriflavine and CpG, designed as tumor vaccines for anticancer therapy. The aggravated hypoxic survival signaling following photodynamic therapy was mitigated by acriflavine, inhibiting HIF-1 $\alpha$ -mediated metastasis and survival. The presence of CpG adjuvants enabled tumor-associated antigens, generated post-photodynamic therapy, to act as tumor vaccines, thereby enhancing antitumor immune responses.<sup>211</sup>

### 5.3. Other types of MOF

A zinc–carnosine MOF was fabricated for CpG adsorption and ovalbumin encapsulation, exhibiting high biocompatibility and potential as the nanoplatform for recombinant protein-based vaccines.<sup>212</sup> Lin and colleagues synthesized a cationic nanoscale MOF (W-5,10,15,20-tetra(*p*-benzoato)porphyrin),

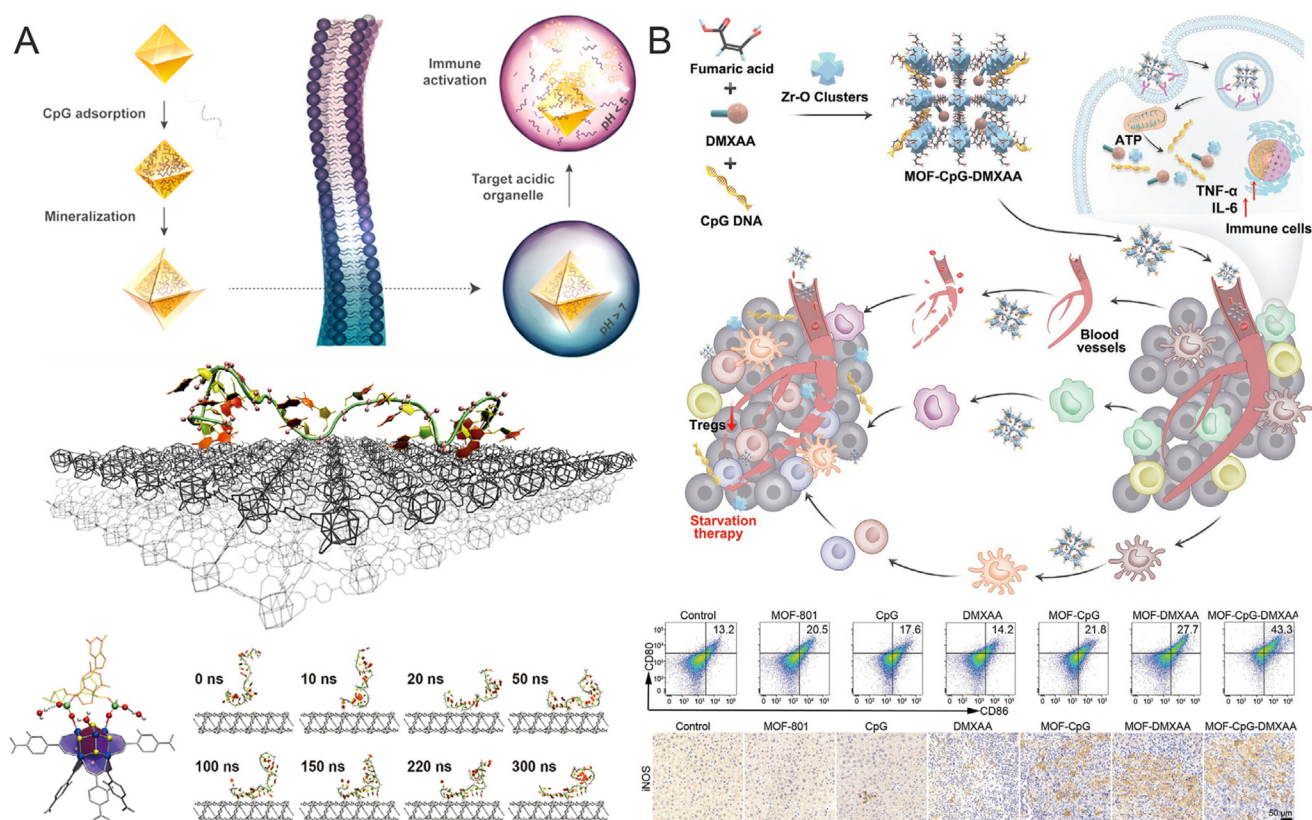


**Fig. 6** (A) Schematic drawing of the MOFs entering into the cells. Illustration of the CpG–MOF complex structure in detail. Snapshots of the process of CpG immobilization.<sup>208</sup> Copyright 2017, American Chemical Society. (B) Schematic of the preparation of MOF–CpG–DMXAA and its mechanism for boosting anticancer immunity. MOF–CpG–DMXAA increased the proportion of the CD80<sup>+</sup>CD86<sup>+</sup> subpopulation in F4/80<sup>+</sup> cells, implying that MOF–CpG–DMXAA promoted the infiltration of M1 TAMs in HCC. Immunohistochemical results of iNOS in livers of orthotopic HCC-bearing mice after 8 administrations of MOF–CpG–DMXAA.<sup>217</sup> Copyright 2023, Wiley-VCH.

effectively integrating photodynamic therapy with CpG delivery. The MOF-mediated photodynamic therapy facilitated the release of tumor-associated antigens, while the delivered CpG promoted dendritic cell maturation, leading to significant antitumor efficacy.<sup>213</sup>

Zhang's team developed a pH-responsive MOF-based co-delivery system (GMP/Eu complex) for the efficient delivery of tumor-associated antigens and CpG. The MOFs, loaded with antigens, efficiently released these antigens in the acidic endo/lysosomal environment due to their relatively labile metal-ligand bonds. Furthermore, CpG was introduced to the MOFs through Watson–Crick base pairing, resulting in an efficient antitumor outcome.<sup>214</sup> Ni *et al.* designed nanoscale MOFs (Hf-DBBF-Ir) as locally activable immunotherapeutics. When activated by X-rays, these MOFs effectively generated reactive oxygen species, delivered CpG as pathogen-associated molecular patterns, and released tumor antigens and danger-associated molecular patterns, for *in situ* personalized cancer vaccination. This approach expanded cytotoxic T cells in tumor-draining lymph nodes, reinvigorating the adaptive immune system for local tumor regression.<sup>215</sup> Fan and colleagues developed the imaging-guided cancer photoimmunotherapy system using MOF MIL101-NH<sub>2</sub> as the core nanocarrier, dual-dressed

with the fluorescent and photoacoustic signal donor indocyanine green, and immune adjuvant CpG. The photoimmunotherapy triggered a cold to hot transformation of tumor cells, and achieved superior antitumor efficiency.<sup>216</sup> Finally, Liu's group reported that MOF-801 could serve as a drug delivery nanocarrier for the 5,6-dimethylxanthone-4-acetic acid (DMXAA) STING agonists and CpG ODNs. This self-assembled nanoparticle effectively improved the tumor microenvironment by destroying tumor blood vessels, and promoting dendritic cell maturation, reprogramming tumor-associated macrophages, resulting in excellent immunotherapeutic activity in hepatocellular carcinoma (Fig. 6B).<sup>217</sup>

## 6. Lipid-based CpG delivery systems

Lipid-based delivery nanosystems, representing a significant advancement in drug delivery technology, have seen numerous liposomal drugs approved and many others reaching late-stage clinical development in the United States.<sup>218,219</sup> Lipid-based delivery systems possess a high affinity for cell membranes. They can easily enter the cytoplasm by endocytosis or direct membrane fusion and then release drugs by lipid-phospho-

pid exchange.<sup>220–224</sup> These systems demonstrate a high affinity for cell membranes, facilitating entry into the cytoplasm through direct membrane fusion or endocytosis, followed by drug release *via* lipid–phospholipid exchange.<sup>161,225</sup> Their capability to prolong the circulation lifetime, enhance uptake, promote passive accumulation at disease sites, and sustain therapeutic payload release has led to proposals for using lipid-based nanoparticles to improve the delivery of CpG ODN-based therapeutics.<sup>226</sup>

Interest in lipid-based CpG delivery grew in the early 2000s. Li *et al.* explored the use of liposomes as a co-delivery vehicle to improve the adjuvant CpG activity with HER-2/neu-derived peptide p63-71, aiming to induce a CD8<sup>+</sup> T-cell response. Mice immunized with biofunctionalized liposomes exhibited antigen-specific IFN- $\gamma$  responses, which were significantly stronger than those in mice immunized with p63-71 alone.<sup>227</sup> Yoshizaki *et al.* utilized cationic lipid-introduced pH-sensitive polymer 3-methylglutaryl hyperbranched poly(glycidol)-modified liposomes for efficient antigen and CpG delivery. Comparing two complexation methods, pre-mix and post-mix, they found that post-mix led to higher cellular immune responses, though both methods showed strong antitumor efficiency in tumor-bearing mice compared with conventional liposomes.<sup>228</sup> Kwak and colleagues reported amphiphilic lipid–DNA aggregation hybridized with CpG and pharmaceutical antigen peptides. This base-pairing approach enabled the efficient delivery of immune agents to CD8 $\alpha$ <sup>+</sup> dendritic cells in tumor-draining lymph nodes and effectively induced antigen-specific immune responses for cancer immunotherapy across various cancer types.<sup>229</sup>

Suzuki and team also developed lipid nanoparticles loaded with type-A CpG ODN, significantly suppressing tumor growth by activating CD8 T cells and altering the tumor immune microenvironment. Combining these nanoparticles with anti-PD-1 antibodies further enhanced therapeutic efficacy.<sup>230</sup> Lai *et al.* designed a novel liposomal vaccine, assembling adjuvant CpG and dendritic cell-targeting mannose on the surface of melanoma-specific TRP2<sub>180–188</sub> peptide-loaded liposomes. This formulation effectively enhanced dendritic cell activation. It also reduced regulatory T cells and myeloid-derived suppressor cells while increasing CD8<sup>+</sup> cytotoxic T cells and IFN- $\gamma$  production, thereby amplifying anti-melanoma efficiency in mice.<sup>231</sup>

Lipid-coated inorganic nanoparticles, which constitute the inorganic nanodelivery systems, are complexed with lipid layers carrying CpG. These lipid-coated inorganic nanoparticles, with multifarious decorations, not only enhance the loading capabilities of CpG ODNs but also hold the potential to improve therapeutic delivery. Zhang and colleagues recently developed a vaccine using tumor-derived antigenic microparticles to encapsulate Fe<sub>3</sub>O<sub>4</sub> nanoparticles, which were then tethered with CpG-loaded liposome arrays on their surface. These vaccines demonstrated both lymph node draining and tumor-targeting capabilities. Remarkably, the Fe<sub>3</sub>O<sub>4</sub> nanoparticles within the vaccines induced a significant infiltration of cytotoxic T lymphocytes and facilitated the reprogramming of infiltrated tumor-associated macrophages into a tumor-suppressive M1 phenotype. Additionally, the combination of these vaccines

with immune checkpoint PD-L1 blockade significantly amplified the immunotherapy effect across multiple established tumor models, highlighting the critical role of spatiotemporal consistency in tumor microenvironment immunomodulation and host immunity (Fig. 7A).<sup>232</sup> In another approach, Gao and colleagues synthesized lipid-coated iron oxide nanoparticles as the nanovaccine to co-deliver adjuvant CpG and peptide antigen into the lysosomes and cytosol of dendritic cells *via* both endosome-mediated endocytosis and membrane fusion. This dual uptake mechanism synergistically stimulated dendritic cell maturation. The iron oxide nanoparticles, generating intracellular reactive oxygen species, also served as adjuvants to further activate immature dendritic cells. The nanovaccine significantly increased antigen-specific T cells, leading to improved animal survival and inhibited tumor growth (Fig. 7B).<sup>233</sup>

## 7. Protein- and peptide-based CpG delivery systems

Natural biomolecules, such as proteins and peptides, are attractive alternatives for CpG delivery owing to their advantages, such as biocompatibility and biodegradability. In addition, peptides composed of programmable amino acids can be designed to enhance many functions, such as stability, selective targeting and barrier protection. Wang's group designed a viral-mimicking vaccine nanoplatfrom using the nonviral E2 core of pyruvate dehydrogenase. This platform is capable of encapsulating CpG and SIINFEKL peptides. The vaccine nanoplatfrom for the concurrent temporal and spatial delivery of CpG and SIINFEKL peptides to DCs led to prolonged and enhanced CD8 T-cell activation.<sup>234</sup> Butkovich *et al.* also constructed nanovaccines based on the E2 protein nanoplatfrom, efficiently delivering CpG1018 or CpG1826 to activate dendritic cells for antigen presentation.<sup>235</sup> Schwendeman and colleagues developed lipoprotein nanodiscs comprised of phospholipids and apolipoprotein A1-mimetic peptides. These nanodiscs, ideally suited for coupling with tumor neoantigen peptides and cholesterol–CpG adjuvants, formed an efficient neoantigen nanovaccine system. The nanodiscs facilitated the co-delivery of antigen and CpG to the lymph nodes, prolonged antigen presentation, and elicited significant antitumor T-cell responses, effectively inhibiting tumor growth.<sup>236</sup> Chen and coworkers created promising albumin/albumin-binding vaccine nanocomplexes for cancer immunotherapy. These nanocomplexes, assembled *in vivo* with endogenous albumin, efficiently delivered antigens and CpG into lymph nodes. They induced approximately ten times more CD8<sup>+</sup> cytotoxic T lymphocytes and inhibited the tumor progression in multiple cancer models (Fig. 8A).<sup>237</sup> Silk fibroin could serve as an effective CpG carrier, stimulating significantly higher levels of immune cytokines and nitric oxide compared with CpG alone.<sup>238</sup> In addition, silk protein was also modified with a nucleic acid-binding domain, poly-lysine, for CpG–STAT3 siRNA delivery. This modification protected CpG–siRNA from degradation and enhanced its internalization by TLR9-positive



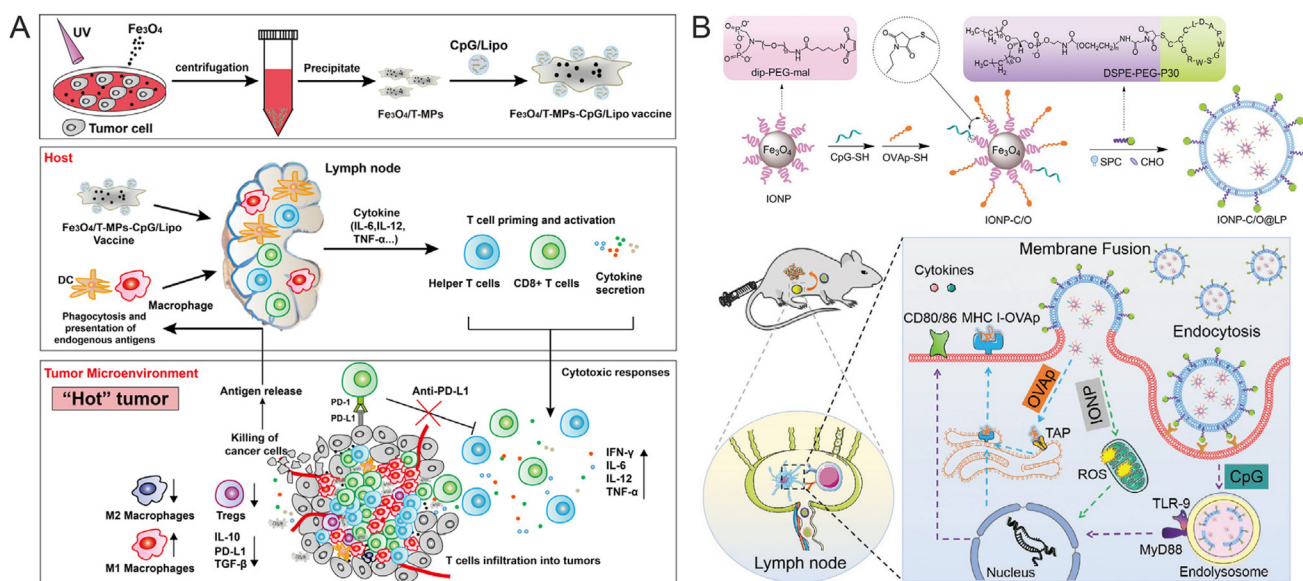


**Fig. 7** (A) Nano-Fe<sub>3</sub>O<sub>4</sub>-carried tumor-derived antigenic microparticles surface-decorated with CpG-loaded liposomes to yield an anticancer vaccine, promoting APC maturation, activating tumor-specific T cells, increasing pro-inflammatory cytokine production, and remodeling the tumor microenvironment to boost antitumor responses to immunotherapy.<sup>232</sup> Copyright 2019, American Chemical Society. (B) Schematic illustration showing the synergistic effects and immune responses elicited by lipid-coated iron oxide nanoparticles for the co-delivery of peptide antigen and CpG.<sup>233</sup> Copyright 2022, Wiley-VCH.

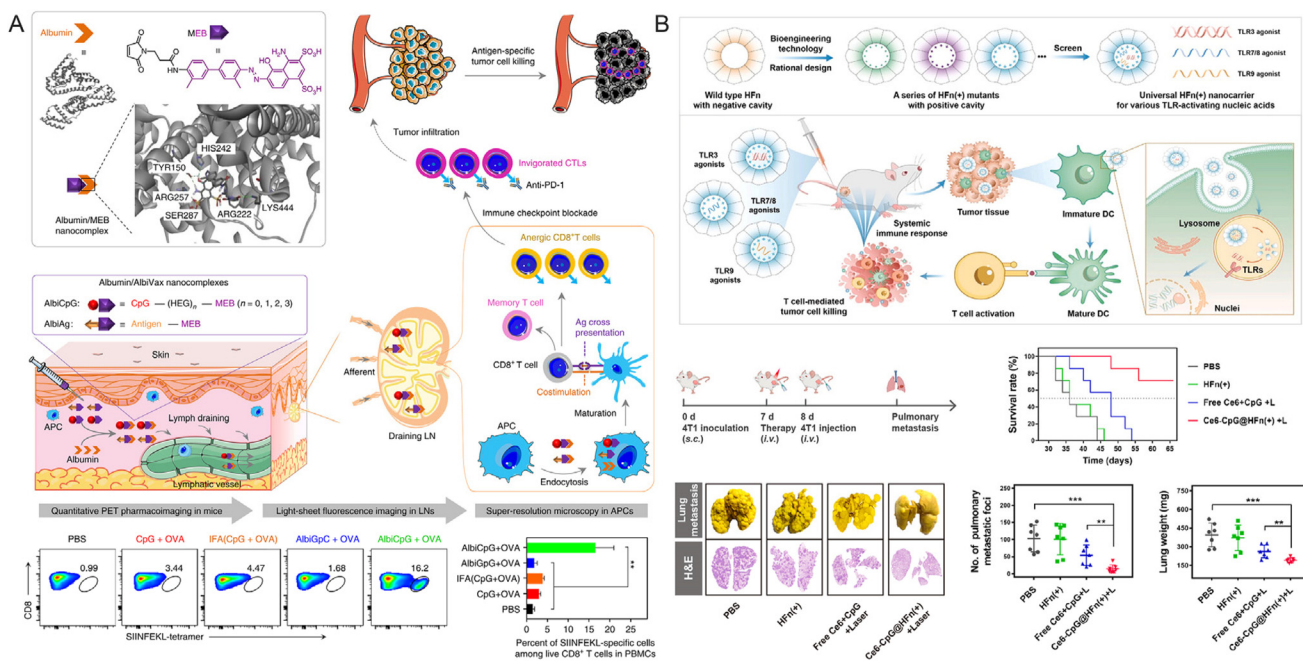


**Fig. 8** (A) Schematic of albumin/AlbiVax nanocomplexes for efficient vaccine delivery and combination cancer immunotherapy. Representative flow cytometry plots and frequency of SIINFEKL<sup>+</sup>CD8<sup>+</sup> T cells in peripheral blood on day 21 stained using phycoerythrin (PE)-labeled H-2Kb-SIINFEKL tetramer.<sup>237</sup> Copyright 2017, Springer Nature. (B) The illustration of the design and screening of a nanocage-based universal carrier for TLR-activating nucleic acids to enhance antitumor immunotherapy. The anti-metastasis efficacy of Ce6-CpG@HFn(+)-based PDT-immunotherapy *in vivo*.<sup>242</sup> Copyright 2022, Elsevier.

macrophages. Silk sphere-encapsulated CpG-STAT3 siRNA exhibited prolonged target gene silencing and improved immunotherapeutic effects *in vivo*.<sup>239</sup>

Wang and colleagues reported a straightforward and effective strategy for peptide vaccination, leveraging non-covalent interactions between cell-penetrating peptide-linked

epitopes and CpG. This co-assembled nanovaccine facilitated rapid endocytosis and substantially enhanced antigen cross-presentation and dendritic cell activation, eliciting strong effector and central memory Th1 and CD8<sup>+</sup> T-cell responses, yielding significant therapeutic effects against melanoma tumors.<sup>240</sup> Chen's group employed flash nanocomplexation technology to create CpG adjuvant nanoparticles. These nanoparticles redirected CpG into the draining lymph nodes. When combined with ovalbumin and influenza H1N1 hemagglutinin antigen, the CpG adjuvant nanoparticles elicited robust cellular and humoral immunity for tumor inhibition and influenza prevention in mice.<sup>241</sup> Lastly, Fan and colleagues bioengineered human heavy-chain ferritin with a positively charged cavity to create optimal nanocarriers for CpG encapsulation *via* electrostatic interaction. This nanocarrier improved the CpG delivery efficiency and enhanced immune activation. Additionally, the photosensitizer chlorin e6 was conjugated on the external surface of the nanocarrier, synergizing immunogenic death inducer-mediated and CpG-mediated immune activation for effective antitumor therapy (Fig. 8B).<sup>242</sup>

## 8. Exosomes

Exosomes are excellent carriers for loading exogenous CpG cargoes, effectively mitigating the challenges associated with the negative charge, hydrophilicity, and relatively large size of

CpG. Exosomes are extracellular vesicles of 30 to 150 nm in diameter that have the same topology as the cell and are enriched in selected proteins, lipids, nucleic acids, and glyco-conjugates. Compared with traditional drug delivery systems, exosomes exhibit unique biocompatibility, can enhance blood circulation half-lives and improve accumulation at targeted sites, thereby increasing the efficiency of immunotherapy.<sup>243</sup> In 2016, Takahashi's group developed a co-delivery nanosystem for tumor antigens and immunostimulatory CpG adjuvant using genetically engineered tumor cell-derived exosomes. They transfected B16BL6 cells with the plasmid vector encoding the fusion streptavidin-lactadherin protein. The resulting genetically engineered streptavidin-lactadherin-expressing exosomes could be combined with biotinylated CpG, effectively activating DC2.4 cells and enhancing tumor antigen presentation. The CpG-modified exosomes demonstrated strong anti-tumor effects in B16BL6 tumor-bearing mice, highlighting its potential for cancer immunotherapy.<sup>244</sup> Takahashi and colleagues also utilized small extracellular vesicles (EVs) for CpG and ovalbumin delivery in treating allergic rhinitis. Intranasal administration of CpG-ovalbumin-EVs significantly raised ovalbumin-specific IgG antibody titers, efficiently alleviating allergic symptoms.<sup>245</sup> Zhao *et al.* created cancer cell apoptotic body-encapsulated CpG ODNs as cancer vaccines for enhanced immunotherapy.<sup>246</sup> Recently, Nie and colleagues designed engineered cellular nanovesicles with immune-reprogramming and tumor-homing biofunctions for photoacoustic imaging-

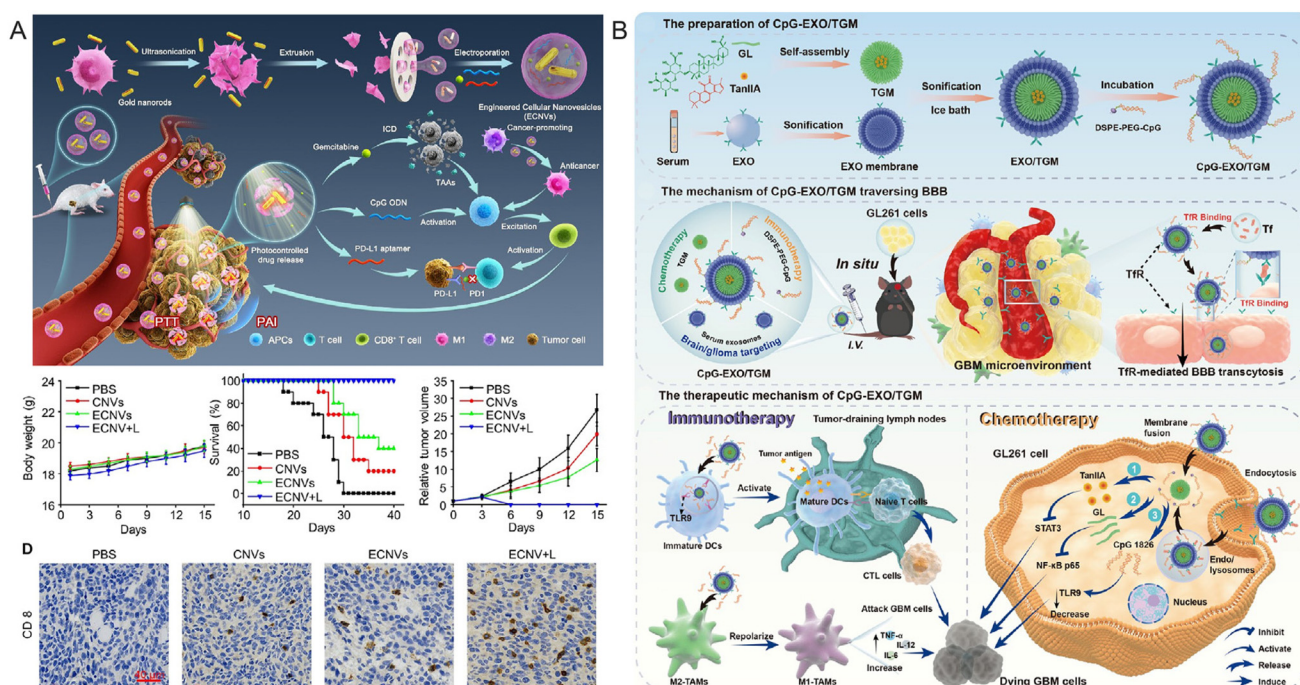


**Fig. 9** (A) Schematic illustration of engineered cellular nanovesicles for photoacoustic imaging-guided phototriggered precision chemoimmunotherapy. The engineered cellular nanovesicles inhibited tumor growth *in vivo*.<sup>247</sup> Copyright 2022, American Chemical Society. (B) Schematic illustration of the preparation and therapeutic mechanism of the CpG anchored on the exosome membrane loaded with traditional Chinese medicine self-assembled nanomicelles.<sup>248</sup> Copyright 2023, American Chemical Society.

directed chemo-immunotherapy. M1-macrophage-derived cellular nanovesicles, loaded with gemcitabine, gold nanorods, PD-L1 aptamer, and CpG, triggered tumor immunogenic cell death with gemcitabine and improved the immune response to antigens released by this cell death with CpG, resulting in a long-term antitumor immunotherapeutic effect. By relieving the inhibitory effect of the PD1/PD-L1 checkpoint, the PD-L1 aptamer additionally relieved the inhibitory effect, augmenting the immune responses (Fig. 9A).<sup>247</sup> Furthermore, a biomimetic brain-targeting delivery nanoplatform based on endogenous serum exosomes was prepared. This platform co-delivered the drug tanshinone IIA, glycyrrhizic acid nanomicelles, and CpG for effective and safe chemo-immunotherapy against glioblastoma. The notable anti-glioblastoma effect of this nanoplatform was attributed to its sufficient intracellular drug release to induce apoptosis of glioblastoma cells, and the induction of macrophage polarization and the stimulation of DC maturation by CpG to activate the anti-glioblastoma immunotherapeutic effect (Fig. 9B).<sup>248</sup>

## 9. Cell membrane

Cell membranes can also be extruded or sonicated to make nanoscale vesicles, which have a unique multicomponent feature, comprising lipids, proteins, and carbohydrates. Zhang and colleagues developed a biomimetic anticancer nanovaccine by encapsulating CpG into biodegradable PLGA nanoparticle cores and coating them with B16-F10 mouse melanoma cells for antitumor immunotherapy. This nanovaccine, when used in conjunction with checkpoint blockades, proved a substantial therapeutic effect (Fig. 10A).<sup>249</sup> The same group also created an adjuvanted nanotoxoid vaccine, leveraging the natural binding interaction of macrophages with protective antigen anthrax toxins. This vaccine, which combined macrophage membrane-coated CpG nanoparticles with anthrax toxins, elicited long-term immunity against anthrax toxins in a murine model even with a single low-dose vaccination (Fig. 10B).<sup>250</sup> Tian and coworkers constructed a nanovaccine by coextruding CD47 knockout/calreticulin dual-bioengineered

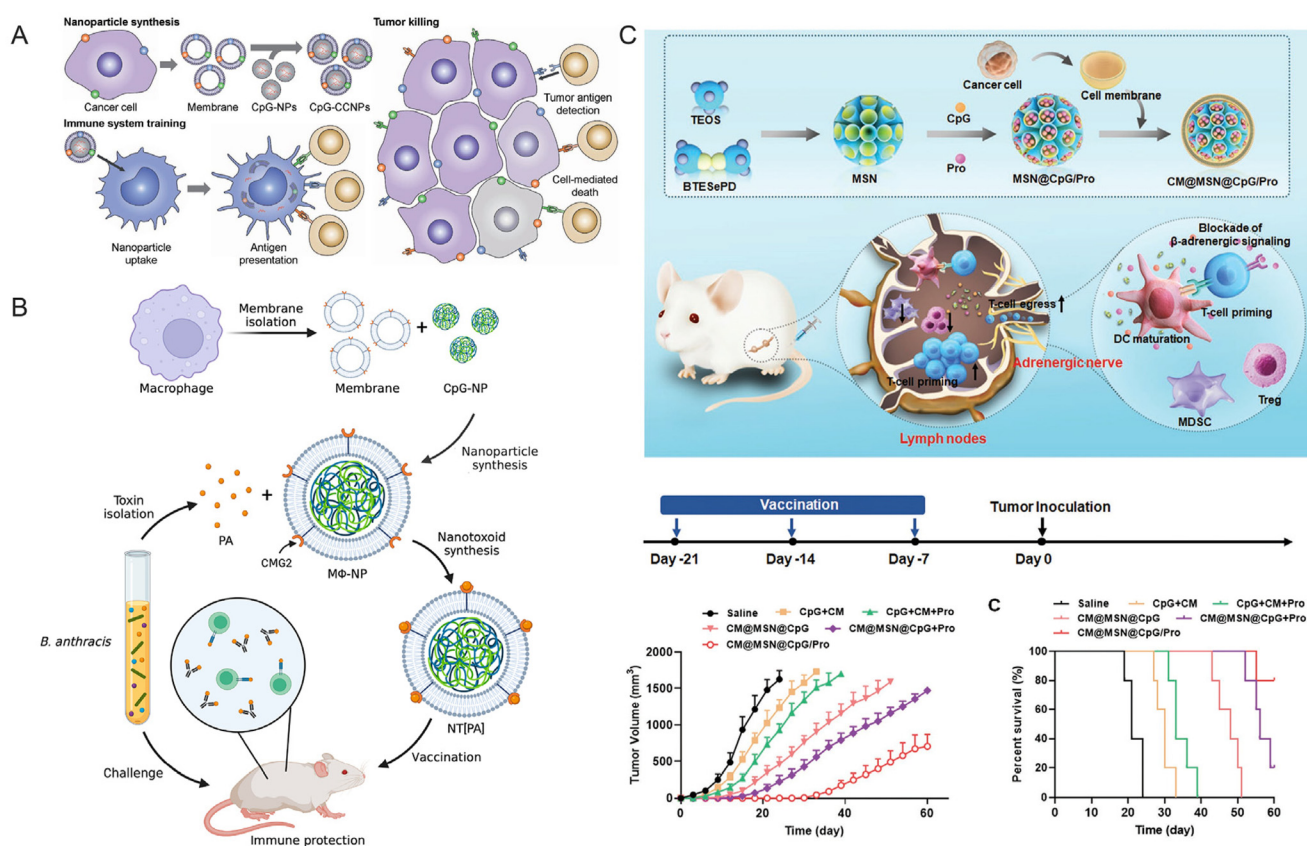


**Fig. 10** (A) Schematic of CpG oligodeoxynucleotide-coated cancer cell-derived nanoparticle vaccines for anticancer vaccination. Membrane derived from cancer cells, along with the associated tumor antigens, is coated onto adjuvant-loaded nanoparticle cores to yield a nanoparticulate anticancer vaccine.<sup>249</sup> Copyright 2017, Wiley-VCH. (B) Nanotoxoids for protection against anthrax. Macrophage membrane-coated nanoparticles are fabricated by coating macrophage membrane expressing the anthrax receptor CMG2 onto polymeric CpG-loaded nanoparticle cores. NPs are then complexed with anthrax toxin protective antigen to form nanotoxoids.<sup>250</sup> Copyright 2022, American Chemical Society. (C) Biomimetic nanovaccine that integrates a blockade of  $\beta$ -adrenergic signaling for enhanced immunotherapy and protection against cancer through improving the priming of the naive CD8<sup>+</sup> T cells and effector T cell egress from lymph nodes as well as decreasing the frequency of immunosuppressive cells in the tumor microenvironment. Prophylactic and therapeutic effects in B16-F10 murine models.<sup>253</sup> Copyright 2023, Wiley-VCH.

B16F10 cell membranes with PEI25k/CpG adjuvant. This nanovaccine enhanced the endocytosis of adjuvants and antigens, inducing the maturation of DCs. The combined use of this nanovaccine with an anti-PD-L1 antibody significantly reduced tumor growth.<sup>251</sup> A “Trojan horse” cancer cell membrane nanovaccine was also devised, utilizing mannose-targeting CpG-layered double hydroxide nanoparticles and a bovine serum albumin coating strategy to overcome immune escape. The “Trojan horse” nanovaccine efficiently targeted APCs for APC maturation, significantly suppressing tumor growth *in vivo*.<sup>252</sup> Wang *et al.* also designed a cancer cell membrane-coated nanovaccine for CpG and  $\beta$ -adrenergic receptor blocker propranolol delivery. This biomimetic nanovaccine efficiently induced antigen presentation and dendritic cell maturation. The integration of  $\beta$ -adrenergic receptor signaling blockade with vaccination enhanced effector T cell egress from lymph nodes and naive CD8<sup>+</sup> T cell priming, while also diminishing the immunosuppressive tumor microenvironment. This led to promoted tumor NK cell and B cell infiltration, resulting in remarkable therapeutic efficacy in B16-F10 melanoma mice (Fig. 10C).<sup>253</sup> In addition to cancer cell membranes, Mangalmurti's group demonstrated that red blood cells (RBCs) could act as critical immune sensors through surface CpG expression. CpG-carrying RBCs drove innate immune activation. During CpG-induced inflammation and polymicrobial sepsis, the erythroid-specific deletion of TLR9 reduced erythrophagocytosis and decreased local and systemic cytokine production, showing RBCs' action as immune sentinels during pathological states.<sup>254</sup>

## 10. Conclusions and future perspectives

CpG ODNs are recognized as the pathogen-associated molecular pattern, triggering a ‘danger signal’ response *via* the TLR9 in vertebrate immune systems. This interaction between CpG and TLR9 initiates a series of immune responses encompassing both innate and acquired immunities. Extensive pre-clinical and clinical evaluations have highlighted the potential of CpG ODNs as versatile immune response modifiers, finding applications as stand-alone immunotherapeutic agents, vaccine adjuvants, and treatments for infectious diseases, allergies, and cancers. However, free CpG ODNs face significant challenges that limit their clinical utility, such as susceptibility to nuclease degradation, inefficient cellular uptake, and lack of specificity towards target cells. The advent of nanomaterial-based systems for CpG delivery has addressed many of these issues. These nanosystems offer an effective means of protecting CpG ODNs from enzymatic digestion, enhancing cellular uptake, and directing the ODNs to specific target cells. This review paper concentrates on the development of nanomaterial-based CpG delivery systems, exploring their role in augmenting the immunotherapeutic efficacy of CpG ODNs.

Despite significant progress in the development of various nanomaterial-based CpG delivery nanoplatfoms for immunotherapy, several challenges remain to be addressed:

(1) While numerous studies have demonstrated the potential of nanomaterial-based delivery systems to greatly enhance the immune activity of CpG ODNs, a comprehensive understanding of the mechanisms underlying this enhanced immunostimulatory activity is still lacking. Investigating the molecular mechanisms of CpG ODN sequences' interaction with receptors and the resultant immunomodulatory functions of nanomaterials is crucial. This research will not only advance immunotherapeutic applications but also contribute to a deeper understanding of immunobiology.

(2) The benefits of nanomaterial-based CpG delivery are manifold, and the exploitation of safe CpG delivery nanosystems is rapidly advancing. Consequently, there is a pressing need to develop new nanomaterials for CpG delivery that exhibit minimal cytotoxicity, improve the efficiency of CpG ODN delivery, and possess additional biofunctions. Such advancements will expand the immunotherapeutic applications of CpG ODNs.

(3) Strategies that are effective in laboratory research often do not directly translate into successful clinical trials or human therapies, which are essential to determine the clinical utility of nanomaterial-based CpG delivery systems. Hence, there is an expectation for the development of clinically applicable nanomaterial-based CpG delivery systems with good stability and biocompatibility under practical operating conditions in the future.

While numerous challenges still need to be overcome, the future holds significant potential for further scientific research and development in the field of nanomaterial-based CpG delivery systems for immunotherapeutic applications.

## Conflicts of interest

There are no conflicts to declare.

## Acknowledgements

This work is supported by the National Key Research and Development Program of China (2019YFA0111300), the National Natural Science Foundation of China (22277155, 52373166), the Science and Technology Program of Guangzhou (2024A04J6572), the Guangdong Provincial Pearl Talents Program (2019QN01Y131), the Thousand Talents Plan, and the China Primary Health Care Foundation (2022-003).

## References

- 1 A. M. Krieg, A.-K. Yi, S. Matson, T. J. Waldschmidt, G. A. Bishop, R. Teasdale, G. A. Koretzky and D. M. Klinman, *Nature*, 1995, **374**, 546–549.
- 2 H. Hemmi, O. Takeuchi, T. Kawai, T. Kaisho, S. Sato, H. Sanjo, M. Matsumoto, K. Hoshino, H. Wagner, K. Takeda and S. Akira, *Nature*, 2000, **408**, 740–745.

- 3 L. Klimek, M. F. Bachmann, G. Senti and T. M. Kundig, *Expert Rev. Clin. Immunol.*, 2014, **10**, 1059–1067.
- 4 F. Wu, X.-Y. Yuan, J. Li and Y.-H. Chen, *Vaccine*, 2009, **27**, 4320–4324.
- 5 H.-A. Kim, H.-M. Ko, H.-W. Ju, K.-J. Kim, S.-G. Roh, H.-K. Lee and S.-Y. Im, *Cancer Lett.*, 2009, **274**, 160–164.
- 6 D. M. Klinman, *Nat. Rev. Immunol.*, 2004, **4**, 249–259.
- 7 P. J. Olbert, A. J. Schrader, C. Simon, A. Dalpke, P. Barth, R. Hofmann and A. Hegele, *Anticancer Res.*, 2009, **29**, 2067–2076.
- 8 S. Nierkens, M. H. den Brok, Z. Garcia, S. Togher, J. Wagenaars, M. Wassink, L. Boon, T. J. Ruers, C. G. Figdor, S. P. Schoenberger, G. J. Adema and E. M. Janssen, *Cancer Res.*, 2011, **71**, 6428–6437.
- 9 M. Yamamoto, T. Sato, J. Beren, D. Verthelyi and D. M. Klinman, *Biomaterials*, 2011, **32**, 4238–4242.
- 10 Z. Huang, Z. Zhang, Y. Jiang, D. Zhang, J. Chen, L. Dong and J. Zhang, *J. Controlled Release*, 2012, **158**, 286–292.
- 11 S. Nechaev, C. Gao, D. Moreira, P. Swiderski, A. Jozwiak, C. M. Kowolik, J. Zhou, B. Armstrong, A. Raubitschek, J. J. Rossi and M. Kortylewski, *J. Controlled Release*, 2013, **170**, 307–315.
- 12 M. Liu, R. S. O'Connor, S. Trefely, K. Graham, N. W. Snyder and G. L. Beatty, *Nat. Immunol.*, 2019, **20**, 265–275.
- 13 C. Caudill, J. L. Perry, K. Iliadis, A. T. Tessema, B. J. Lee, B. S. Mecham, S. Tian and J. M. DeSimone, *Proc. Natl. Acad. Sci. U. S. A.*, 2021, **118**, e2102595118.
- 14 A. M. Krieg, *Nat. Rev. Drug Discovery*, 2006, **5**, 471–484.
- 15 N. Hanagata, *Int. J. Nanomed.*, 2017, **12**, 515–531.
- 16 J. Vollmer and A. M. Krieg, *Adv. Drug Delivery Rev.*, 2009, **61**, 195–204.
- 17 G. Mutwiri, S. van Drunen Littel-van den Hurk and L. A. Babiuk, *Adv. Drug Delivery Rev.*, 2009, **61**, 226–232.
- 18 P. Yousefpour, K. Ni and D. J. Irvine, *Nat. Rev. Bioeng.*, 2023, **1**, 107–124.
- 19 F. Meng, J. Wang and Y. Yeo, *J. Controlled Release*, 2022, **345**, 586–600.
- 20 J. Tan, B. Ding, B. Teng, P. Ma and J. Lin, *Adv. Funct. Mater.*, 2022, **32**, 2111670.
- 21 F. Ding, S. Zhang, Q. Chen, H. Feng, Z. Ge, X. Zuo, C. Fan, Q. Li and Q. Xia, *Small*, 2023, **19**, 2206228.
- 22 X. Ma, S.-J. Li, Y. Liu, T. Zhang, P. Xue, Y. Kang, Z.-J. Sun and Z. Xu, *Chem. Soc. Rev.*, 2022, **51**, 5136–5174.
- 23 Y. Tao, H. F. Chan, B. Shi, M. Li and K. W. Leong, *Adv. Funct. Mater.*, 2020, **30**, 2005029.
- 24 M. Roman, E. Martin-Orozco, J. S. Goodman, M.-D. Nguyen, Y. Sato, A. Ronaghy, R. S. Kornbluth, D. D. Richman, D. A. Carson and E. Raz, *Nat. Med.*, 1997, **3**, 849–854.
- 25 A. K. Salem and G. J. Weiner, *Adv. Drug Delivery Rev.*, 2009, **61**, 193–194.
- 26 E. Latz, A. Schoenemeyer, A. Visintin, K. A. Fitzgerald, B. G. Monks, C. F. Knetter, E. Lien, N. J. Nilsen, T. Espevik and D. T. Golenbock, *Nat. Immunol.*, 2004, **5**, 190–198.
- 27 M. V. Lasker and S. K. Nair, *J. Immunol.*, 2006, **177**, 11–16.
- 28 G. M. Barton, J. C. Kagan and R. Medzhitov, *Nat. Immunol.*, 2006, **7**, 49–56.
- 29 K. K. L. Phua, H. F. Staats, K. W. Leong and S. K. Nair, *Sci. Rep.*, 2014, **4**, 5128.
- 30 D.-W. Yeh, Y.-L. Liu, Y.-C. Lo, C.-H. Yuh, G.-Y. Yu, J.-F. Lo, Y. Luo, R. Xiang and T.-H. Chuang, *Proc. Natl. Acad. Sci. U. S. A.*, 2013, **110**, 20711–20716.
- 31 K. K. Phua, S. K. Nair and K. W. Leong, *Nanoscale*, 2014, **6**, 7715–7729.
- 32 E. Latz, A. Verma, A. Visintin, M. Gong, C. M. Sirois, D. C. G. Klein, B. G. Monks, C. J. McKnight, M. S. Lamphier, W. P. Duprex, T. Espevik and D. T. Golenbock, *Nat. Immunol.*, 2007, **8**, 772–779.
- 33 G. M. Barton and R. Medzhitov, *Science*, 2003, **300**, 1524–1525.
- 34 P. Tailor, T. Tamura and K. Ozato, *Cell Res.*, 2006, **16**, 134–140.
- 35 H. Xu, H. An, Y. Yu, M. Zhang, R. Qi and X. Cao, *J. Biol. Chem.*, 2003, **278**, 36334–36340.
- 36 A. M. Krieg, *Annu. Rev. Immunol.*, 2002, **20**, 709–760.
- 37 C. Schetter and J. Vollmer, *Curr. Opin. Drug Discovery Dev.*, 2004, **7**, 204–210.
- 38 G. J. Weiner, H. M. Liu, J. E. Wooldridge, C. E. Dahle and A. M. Krieg, *Proc. Natl. Acad. Sci. U. S. A.*, 1997, **94**, 10833–10837.
- 39 G. Strandskog, I. Skjæveland, T. Ellingsen and J. B. Jørgensen, *Vaccine*, 2008, **26**, 4704–4715.
- 40 G. Mutwiri, P. Benjamin, H. Soita and L. A. Babiuk, *Vaccine*, 2008, **26**, 2680–2688.
- 41 A. K. Yi, J. H. Chace, J. S. Cowdery and A. M. Krieg, *J. Immunol.*, 1996, **156**, 558–564.
- 42 S. Kuwajima, T. Sato, K. Ishida, H. Tada, H. Tezuka and T. Ohteki, *Nat. Immunol.*, 2006, **7**, 740–746.
- 43 Y. Liu, X. Luo, C. Yang, S. Yu and H. Xu, *Vaccine*, 2011, **29**, 5778–5784.
- 44 S. M. Singh, T. N. Alkie, D. C. Hodgins, É. Nagy, B. Shojadoost and S. Sharif, *Vaccine*, 2015, **33**, 3947–3952.
- 45 N. Hanagata, *Int. J. Nanomed.*, 2012, **7**, 2181–2195.
- 46 B. Badie and J. M. Berlin, *Immunotherapy*, 2012, **5**, 1–3.
- 47 A. H. Dalpke, S. Zimmermann, I. Albrecht and K. Heeg, *Immunology*, 2002, **106**, 102–112.
- 48 G. Hartmann, R. D. Weeratna, Z. K. Ballas, P. Payette, S. Blackwell, I. Suparto, W. L. Rasmussen, M. Waldschmidt, D. Sajuthi, R. H. Purcell, H. L. Davis and A. M. Krieg, *J. Immunol.*, 2000, **164**, 1617–1624.
- 49 G. Hartmann and A. M. Krieg, *J. Immunol.*, 2000, **164**, 944–953.
- 50 A. Krug, A. Towarowski, S. Britsch, S. Rothenfusser, V. Hornung, R. Bals, T. Giese, H. Engelmann, S. Endres, A. M. Krieg and G. Hartmann, *Eur. J. Immunol.*, 2001, **31**, 3026–3037.
- 51 H. Poeck, M. Wagner, J. Battiany, S. Rothenfusser, D. Wellisch, V. Hornung, B. Jahrsdorfer, T. Giese, S. Endres and G. Hartmann, *Blood*, 2003, **103**, 3058–3064.
- 52 J. Vollmer, R. Weeratna, P. Payette, M. Jurk, C. Schetter, M. Laucht, T. Wader, S. Tluk, M. Liu, H. L. Davis and A. M. Krieg, *Eur. J. Immunol.*, 2004, **34**, 251–262.

- 53 U. Samulowitz, M. Weber, R. Weeratna, E. Uhlmann, B. Noll, A. M. Krieg and J. Vollmer, *Oligonucleotides*, 2010, **20**, 93–101.
- 54 E. Kandimalla and S. Agrawal, in *Nucleic Acid Drugs*, ed. A. Murakami, Springer Berlin Heidelberg, 2012, ch. 138, vol. 249, pp. 61–93.
- 55 S. Surana, A. R. Shenoy and Y. Krishnan, *Nat. Nanotechnol.*, 2015, **10**, 741–747.
- 56 Q. Jiang, C. Song, J. Nangreave, X. Liu, L. Lin, D. Qiu, Z. G. Wang, G. Zou, X. Liang, H. Yan and B. Ding, *J. Am. Chem. Soc.*, 2012, **134**, 13396–13403.
- 57 M. Komiyama, N. Shigi and K. Ariga, *Adv. Funct. Mater.*, 2022, **32**, 2200924.
- 58 M. H. Teplensky, M. Evangelopoulos, J. W. Dittmar, C. M. Forsyth, A. J. Sinegra, S. Wang and C. A. Mirkin, *Nat. Biomed. Eng.*, 2023, **19**, 911–927.
- 59 H. Wei, F. Li, T. Xue, H. Wang, E. Ju, M. Li and Y. Tao, *Bioact. Mater.*, 2023, **28**, 50–60.
- 60 R. Tian, Y. Shang, Y. Wang, Q. Jiang and B. Ding, *Small Methods*, 2023, **7**, 2201518.
- 61 E. R. Kandimalla, L. Bhagat, Y.-P. Cong, R. K. Pandey, D. Yu, Q. Zhao and S. Agrawal, *Biochem. Biophys. Res. Commun.*, 2003, **306**, 948–953.
- 62 K. Hoshi, T. Yamazaki, Y. Sugiyama, K. Tsukakoshi, W. Tsugawa, K. Sode and K. Ikebukuro, *Nucleic Acid Ther.*, 2019, **29**, 224–229.
- 63 M. Nishikawa, M. Matono, S. Rattanakiat, N. Matsuoka and Y. Takakura, *Immunology*, 2008, **124**, 247–255.
- 64 K. Mohri, M. Nishikawa, N. Takahashi, T. Shiomi, N. Matsuoka, K. Ogawa, M. Endo, K. Hidaka, H. Sugiyama, Y. Takahashi and Y. Takakura, *ACS Nano*, 2012, **6**, 5931–5940.
- 65 Y. Takahashi, T. Maezawa, Y. Araie, Y. Takahashi, Y. Takakura and M. Nishikawa, *J. Pharm. Sci.*, 2017, **106**, 2457–2462.
- 66 Y. Qu, Y. Ju, C. Cortez-Jugo, Z. Lin, S. Li, J. Zhou, Y. Ma, A. Glab, S. J. Kent, F. Cavalieri and F. Caruso, *Small*, 2020, **16**, 2002750.
- 67 Y. Qu, R. De Rose, C.-J. Kim, J. Zhou, Z. Lin, Y. Ju, S. K. Bhangu, C. Cortez-Jugo, F. Cavalieri and F. Caruso, *Angew. Chem., Int. Ed.*, 2023, **62**, e202214935.
- 68 S. Rattanakiat, M. Nishikawa, H. Funabashi, D. Luo and Y. Takakura, *Biomaterials*, 2009, **30**, 5701–5706.
- 69 K. Mohri, E. Kusuki, S. Ohtsuki, N. Takahashi, M. Endo, K. Hidaka, H. Sugiyama, Y. Takahashi, Y. Takakura and M. Nishikawa, *Biomacromolecules*, 2015, **16**, 1095–1101.
- 70 Y. J. Qu, J. J. Yang, P. F. Zhan, S. L. Liu, K. Zhang, Q. Jiang, C. Li and B. Q. Ding, *ACS Appl. Mater. Interfaces*, 2017, **9**, 20324–20329.
- 71 M. E. Distler, J. P. Cavaliere, M. H. Teplensky, M. Evangelopoulos and C. A. Mirkin, *Proc. Natl. Acad. Sci. U. S. A.*, 2023, **120**, e2215091120.
- 72 R. Schlapak, J. Danzberger, D. Armitage, D. Morgan, A. Ebner, P. Hinterdorfer, P. Pollheimer, H. J. Gruber, F. Schäffler and S. Howorka, *Small*, 2012, **8**, 89–97.
- 73 H. Lee, A. K. R. Lytton-Jean, Y. Chen, K. T. Love, A. I. Park, E. D. Karagiannis, A. Sehgal, W. Querbes, C. S. Zurenko, M. Jayaraman, C. G. Peng, K. Charisse, A. Borodovsky, M. Manoharan, J. S. Donahoe, J. Truelove, M. Nahrendorf, R. Langer and D. G. Anderson, *Nat. Nanotechnol.*, 2012, **7**, 389–393.
- 74 R. Crawford, C. M. Erben, J. Periz, L. M. Hall, T. Brown, A. J. Turberfield and A. N. Kapanidis, *Angew. Chem., Int. Ed.*, 2013, **52**, 2284–2288.
- 75 H. Wei, K. Yi, F. Li, D. Li, J. Yang, R. Shi, Y. Jin, H. Wang, J. Ding, Y. Tao and M. Li, *Adv. Mater.*, 2023, 2305826.
- 76 J. Li, H. Pei, B. Zhu, L. Liang, M. Wei, Y. He, N. Chen, D. Li, Q. Huang and C. Fan, *ACS Nano*, 2011, **5**, 8783–8789.
- 77 X. Liu, Y. Xu, T. Yu, C. Clifford, Y. Liu, H. Yan and Y. Chang, *Nano Lett.*, 2012, **12**, 4254–4259.
- 78 J. Cheng, S. Wang, Q. Min, J. Song and Y. Tian, *Colloids Surf., A*, 2022, **637**, 128184.
- 79 M. Liu, L. Hao, D. Zhao, J. Li and Y. Lin, *ACS Appl. Mater. Interfaces*, 2022, **14**, 38506–38514.
- 80 F. Shen, L. Sun, L. Wang, R. Peng, C. Fan and Z. Liu, *Nano Lett.*, 2022, **22**, 4509–4518.
- 81 P. W. K. Rothmund, *Nature*, 2006, **440**, 297–302.
- 82 V. J. Schuller, S. Heidegger, N. Sandholzer, P. C. Nickels, N. A. Suhartha, S. Endres, C. Bourquin and T. Liedl, *ACS Nano*, 2011, **5**, 9696–9702.
- 83 A. Comberlato, M. M. Koga, S. Nüssing, I. A. Parish and M. M. C. Bastings, *Nano Lett.*, 2022, **22**, 2506–2513.
- 84 R. R. Du, E. Cedrone, A. Romanov, R. Falkovich, M. A. Dobrovolskaia and M. Bathe, *ACS Nano*, 2022, **16**, 20340–20352.
- 85 L. Zhang, G. Zhu, L. Mei, C. Wu, L. Qiu, C. Cui, Y. Liu, I. T. Teng and W. Tan, *ACS Appl. Mater. Interfaces*, 2015, **7**, 24069–24074.
- 86 G. Zhu, L. Mei, H. D. Vishwasrao, O. Jacobson, Z. Wang, Y. Liu, B. C. Yung, X. Fu, A. Jin, G. Niu, Q. Wang, F. Zhang, H. Shroff and X. Chen, *Nat. Commun.*, 2017, **8**, 1482.
- 87 C. Wang, W. Sun, G. Wright, A. Z. Wang and Z. Gu, *Adv. Mater.*, 2016, **28**, 8912–8920.
- 88 D. Wang, J. Liu, J. Duan, Y. Ma, H. Gao, Z. Zhang, J. Liu, J. Shi and K. Zhang, *ACS Appl. Mater. Interfaces*, 2022, **14**, 44183–44198.
- 89 H. Wei, Z. Zhao, Y. Wang, J. Zou, Q. Lin and Y. Duan, *ACS Appl. Mater. Interfaces*, 2019, **11**, 46479–46489.
- 90 M. Nishikawa, K. Ogawa, Y. Umeki, K. Mohri, Y. Kawasaki, H. Watanabe, N. Takahashi, E. Kusuki, R. Takahashi, Y. Takahashi and Y. Takakura, *J. Controlled Release*, 2014, **180**, 25–32.
- 91 Y. Umeki, K. Mohri, Y. Kawasaki, H. Watanabe, R. Takahashi, Y. Takahashi, Y. Takakura and M. Nishikawa, *Adv. Funct. Mater.*, 2015, **25**, 5758–5767.
- 92 Y. Umeki, M. Saito, Y. Takahashi, Y. Takakura and M. Nishikawa, *Adv. Healthcare Mater.*, 2017, **6**, 1700355.
- 93 T. Tanifuji, M. Nishimura, K. Kusamori and M. Nishikawa, *J. Controlled Release*, 2023, **354**, 429–438.

- 94 D. Smith, V. Schüller, C. Engst, J. Rädler and T. Liedl, *Nanomedicine*, 2012, **8**, 105–121.
- 95 K. R. Kim, T. Lee, B. S. Kim and D. R. Ahn, *Chem. Sci.*, 2014, **5**, 1533–1537.
- 96 G. Yu, F. Dong, W. Ge, L. Sun, L. Zhang, L. Yuan, N. Li, H. Dai, L. Shi and Y. Wang, *Nano Today*, 2022, **44**, 101498.
- 97 A. S. Walsh, H. Yin, C. M. Erben, M. J. A. Wood and A. J. Turberfield, *ACS Nano*, 2011, **5**, 5427–5432.
- 98 G. D. Hamblin, K. M. Carneiro, J. F. Fakhoury, K. E. Bujold and H. F. Sleiman, *J. Am. Chem. Soc.*, 2012, **134**, 2888–2891.
- 99 M. Bendayan, *Science*, 2001, **291**, 1363–1365.
- 100 M.-C. Daniel and D. Astruc, *Chem. Rev.*, 2004, **104**, 293–346.
- 101 D. A. Giljohann, D. S. Seferos, W. L. Daniel, M. D. Massich, P. C. Patel and C. A. Mirkin, *Angew. Chem., Int. Ed.*, 2010, **49**, 3280–3294.
- 102 C. J. Murphy, A. M. Gole, J. W. Stone, P. N. Sisco, A. M. Alkilany, E. C. Goldsmith and S. C. Baxter, *Acc. Chem. Res.*, 2008, **41**, 1721–1730.
- 103 B. Wang, N. Chen, Y. Wei, J. Li, L. Sun, J. Wu, Q. Huang, C. Liu, C. Fan and H. Song, *Sci. Rep.*, 2012, **2**, 563.
- 104 J. C. Love, L. A. Estroff, J. K. Kriebel, R. G. Nuzzo and G. M. Whitesides, *Chem. Rev.*, 2005, **105**, 1103–1170.
- 105 M. Wei, N. Chen, J. Li, M. Yin, L. Liang, Y. He, H. Song, C. Fan and Q. Huang, *Angew. Chem., Int. Ed.*, 2012, **51**, 1202–1206.
- 106 N. Chen, M. Wei, Y. Sun, F. Li, H. Pei, X. Li, S. Su, Y. He, L. Wang, J. Shi, C. Fan and Q. Huang, *Small*, 2014, **10**, 368–375.
- 107 J. Luo, Y. Cheng, X.-Y. He, Y. Liu, N. Peng, Z.-W. Gong, K. Wu and T. Zou, *Colloids Surf., B*, 2019, **175**, 248–255.
- 108 J. Yue, R. M. Pallares, L. E. Cole, E. E. Coughlin, C. A. Mirkin, A. Lee and T. W. Odom, *ACS Appl. Mater. Interfaces*, 2018, **10**, 21920–21926.
- 109 K. Lee, Z. N. Huang, C. A. Mirkin and T. W. Odom, *Nano Lett.*, 2020, **20**, 6170–6175.
- 110 K. Lee, I. Jung and T. W. Odom, *J. Am. Chem. Soc.*, 2022, **144**, 5274–5279.
- 111 Y. Krishnamachari and A. K. Salem, *Adv. Drug Delivery Rev.*, 2009, **61**, 205–217.
- 112 V. Sokolova, T. Knuschke, A. Kovtun, J. Buer, M. Epple and A. M. Westendorf, *Biomaterials*, 2010, **31**, 5627–5633.
- 113 H. J. Cho, K. Takabayashi, P. M. Cheng, M. D. Nguyen, M. Corr, S. Tuck and E. Raz, *Nat. Biotechnol.*, 2000, **18**, 509–514.
- 114 Z. Li, Z. Liu, M. Yin, X. Yang, J. Ren and X. Qu, *Adv. Healthcare Mater.*, 2013, **2**, 1309–1313.
- 115 I.-H. Lee, H.-K. Kwon, S. An, D. Kim, S. Kim, M. K. Yu, J.-H. Lee, T.-S. Lee, S.-H. Im and S. Jon, *Angew. Chem., Int. Ed.*, 2012, **51**, 8800–8805.
- 116 Y. Tao, E. G. Ju, Z. H. Li, J. S. Ren and X. G. Qu, *Adv. Funct. Mater.*, 2014, **24**, 1004–1010.
- 117 Y. Tao, Y. Zhang, E. Ju, H. Ren and J. Ren, *Nanoscale*, 2015, **7**, 12419–12426.
- 118 Y. Tao, E. Ju, Z. Liu, K. Dong, J. Ren and X. Qu, *Biomaterials*, 2014, **35**, 6646–6656.
- 119 Y. Li, L. H. He, H. Q. Dong, Y. Q. Liu, K. Wang, A. Li, T. B. Ren, D. L. Shi and Y. Y. Li, *Adv. Sci.*, 2018, **5**, 1700805.
- 120 Y. Jia, K. Shi, L. Dai, X. He, H. Deng, R. Han, F. Yang, B. Chu, J. Liao, X. Wei and Z. Qian, *Small Methods*, 2023, **7**, 2201087.
- 121 D. Huang, T. Wu, S. Lan, C. Liu, Z. Guo and W. Zhang, *Biomaterials*, 2022, **289**, 121808.
- 122 J.-H. Han, Y. Y. Lee, H. E. Shin, J. Han, J. M. Kang, C.-P. James Wang, J.-H. Park, S.-N. Kim, J.-H. Yoon, H.-K. Kwon, D.-H. Park, T.-E. Park, Y. B. Choy, D.-H. Kim, T.-H. Kim, J. Min, I.-H. Kim, C. G. Park, D. K. Han and W. Park, *Biomaterials*, 2022, **289**, 121762.
- 123 J. Liu, L. Guo, Z. Mi, Z. Liu, P. Rong and W. Zhou, *J. Controlled Release*, 2022, **348**, 1050–1065.
- 124 Y. Tao, Z. Li, E. Ju, J. Ren and X. Qu, *Chem. Commun.*, 2013, **49**, 6918–6920.
- 125 Y. Tao, Y. Zhang, E. Ju, J. Ren and X. Qu, *Colloids Surf., B*, 2015, **126**, 585–589.
- 126 J. Ming, J. Zhang, Y. Shi, W. Yang, J. Li, D. Sun, S. Xiang, X. Chen, L. Chen and N. Zheng, *Nanoscale*, 2020, **12**, 3916–3930.
- 127 Z. Fu, D. Ni, S. Cai, H. Li, Y. Xiong, R. Yang and C. Chen, *Nano Today*, 2022, **46**, 101590.
- 128 Z. Wang, Y. Zhang, Z. Liu, K. Dong, C. Liu, X. Ran, F. Pu, E. Ju, J. Ren and X. Qu, *Nanoscale*, 2017, **9**, 14236–14247.
- 129 M. He, T. Xiao, Y. Wang, H. Yu, Z. Wang, X. Shi and H. Wang, *Chem. Eng. J.*, 2023, **453**, 139634.
- 130 J.-H. Han, H. E. Shin, J. Lee, J. M. Kang, J.-H. Park, C. G. Park, D. K. Han, I.-H. Kim and W. Park, *Small*, 2022, **18**, 2200316.
- 131 J. Chen, J. Lu, Y. Shan, Y. Wang, Z. Xu, J. Xi, L. Fan and L. Gao, *Adv. Ther.*, 2023, **6**, 2200175.
- 132 L. Guo, D. D. Yan, D. Yang, Y. Li, X. Wang, O. Zalewski, B. Yan and W. Lu, *ACS Nano*, 2014, **8**, 5670–5681.
- 133 L. Chen, L. Zhou, C. Wang, Y. Han, Y. Lu, J. Liu, X. Hu, T. Yao, Y. Lin, S. Liang, S. Shi and C. Dong, *Adv. Mater.*, 2019, **31**, 1904997.
- 134 Q. Han, X. Wang, X. Jia, S. Cai, W. Liang, Y. Qin, R. Yang and C. Wang, *Nanoscale*, 2017, **9**, 5927–5934.
- 135 S. V. Dorozhkin and M. Epple, *Angew. Chem., Int. Ed.*, 2002, **41**, 3130–3146.
- 136 C. Qi, S. Musetti, L. H. Fu, Y. J. Zhu and L. Huang, *Chem. Soc. Rev.*, 2019, **48**, 2698–2737.
- 137 S. Neumann, A. Kovtun, I. D. Dietzel, M. Epple and R. Heumann, *Biomaterials*, 2009, **30**, 6794–6802.
- 138 V. Sokolova, T. Knuschke, J. Buer, A. M. Westendorf and M. Epple, *Acta Biomater.*, 2011, **7**, 4029–4036.
- 139 Z. Xu, Y. Wang, L. Zhang and L. Huang, *ACS Nano*, 2014, **8**, 3636–3645.
- 140 R. Khalifehzadeh and H. Arami, *Nanoscale*, 2020, **12**, 9603–9615.
- 141 Y. Zhai, Y. Dou, D. Zhao, P. F. Fulvio, R. T. Mayes and S. Dai, *Adv. Mater.*, 2011, **23**, 4828–4850.

- 142 Y. Liu, Y. Zhao, B. Sun and C. Chen, *Acc. Chem. Res.*, 2013, **46**, 702–713.
- 143 A. Bianco, J. Hoebeke, S. Godefroy, O. Chaloin, D. Pantarotto, J. P. Briand, S. Muller, M. Prato and C. D. Partidos, *J. Am. Chem. Soc.*, 2005, **127**, 58–59.
- 144 P. C. de Faria, L. I. dos Santos, J. P. Coelho, H. B. Ribeiro, M. A. Pimenta, L. O. Ladeira, D. A. Gomes, C. A. Furtado and R. T. Gazzinelli, *Nano Lett.*, 2014, **14**, 5458–5470.
- 145 Y. Li, Y. Deng, X. Tian, H. Ke, M. Guo, A. Zhu, T. Yang, Z. Guo, Z. Ge, X. Yang and H. Chen, *ACS Nano*, 2015, **9**, 9626–9637.
- 146 Z. Sheng, L. Song, J. Zheng, D. Hu, M. He, M. Zheng, G. Gao, P. Gong, P. Zhang, Y. Ma and L. Cai, *Biomaterials*, 2013, **34**, 5236–5243.
- 147 L. Feng, X. Yang, X. Shi, X. Tan, R. Peng, J. Wang and Z. Liu, *Small*, 2013, **9**, 1989–1997.
- 148 Y. Tao, E. Ju, J. Ren and X. Qu, *Biomaterials*, 2014, **35**, 9963–9971.
- 149 C. Wu, L. Wang, Y. Tian, X. Guan, Q. Liu, S. Li, X. Qin, H. Yang and Y. Liu, *ACS Appl. Mater. Interfaces*, 2018, **10**, 6942–6955.
- 150 I. I. Slowing, B. G. Trewyn, S. Giri and V. S. Y. Lin, *Adv. Funct. Mater.*, 2007, **17**, 1225–1236.
- 151 Z. Li, J. C. Barnes, A. Bosoy, J. F. Stoddart and J. I. Zink, *Chem. Soc. Rev.*, 2012, **41**, 2590–2605.
- 152 F. Tang, L. Li and D. Chen, *Adv. Mater.*, 2012, **24**, 1504–1534.
- 153 S. Chen, Q. Zhang, L. Jia, X. Du and N. Hanagata, *J. Mater. Chem. B*, 2015, **3**, 7246–7254.
- 154 H. Zheng, S. Wen, Y. Zhang and Z. Sun, *PLoS One*, 2015, **10**, e0140265.
- 155 M. An, M. Li, J. C. Xi and H. P. Liu, *ACS Appl. Mater. Interfaces*, 2017, **9**, 23466–23475.
- 156 M. Zhu, X. Ding, R. Zhao, X. Liu, H. Shen, C. Cai, M. Ferrari, H. Y. Wang and R.-F. Wang, *J. Controlled Release*, 2018, **272**, 72–82.
- 157 W. Ngamcherdtrakul, M. Reda, M. A. Nelson, R. Wang, H. Y. Zaidan, D. S. Bejan, N. H. Hoang, R. S. Lane, S.-W. Luoh, S. A. Leachman, G. B. Mills, J. W. Gray, A. W. Lund and W. Yantasee, *Adv. Mater.*, 2021, **33**, 2100628.
- 158 X. Li, G. Chen, Y. Wang, L. Su, B. Chen, K. Wu, Y. Xing, Z. Song, R. Dai, T. Liu, J. Zhao, Z. Xie, P. Zhou, X. Xia and Y. Min, *Nano Res.*, 2022, **15**, 8326–8335.
- 159 X. Zhong, G. Du, X. Wang, Y. Ou, H. Wang, Y. Zhu, X. Hao, Z. Xie, Y. Zhang, T. Gong, Z. Zhang and X. Sun, *Small*, 2022, **18**, 2105530.
- 160 J. Hu and S. Liu, *Acc. Chem. Res.*, 2014, **47**, 2084–2095.
- 161 K. D. Wilson, S. D. de Jong and Y. K. Tam, *Adv. Drug Delivery Rev.*, 2009, **61**, 233–242.
- 162 S. Chen, H. Zhang, X. Shi, H. Wu and N. Hanagata, *Lab Chip*, 2014, **14**, 1842–1849.
- 163 D. Qiao, L. Liu, Y. Chen, C. Xue, Q. Gao, H.-Q. Mao, K. W. Leong and Y. Chen, *Nano Lett.*, 2018, **18**, 3007–3016.
- 164 H. Huang, W. Xie, D. Hu, X. He, R. Li, X. Zhang and Y. Wei, *Chem. Eng. J.*, 2023, **451**, 138617.
- 165 S.-Y. Kim, M. B. Heo, G.-S. Hwang, Y. Jung, D. Y. Choi, Y.-M. Park and Y. T. Lim, *Angew. Chem., Int. Ed.*, 2015, **54**, 8139–8143.
- 166 M. Li, R. Guo, J. Wei, M. Deng, J. Li, Y. Tao, M. Li and Q. He, *Acta Biomater.*, 2021, **136**, 546–557.
- 167 L. Lin, Y. Hu, Z. Guo, J. Chen, P. Sun, H. Tian and X. Chen, *Bioact. Mater.*, 2023, **25**, 689–700.
- 168 G. Catania, G. Rodella, K. Vanvarenberg, V. Pr eat and A. Malfanti, *Biomaterials*, 2023, **294**, 122006.
- 169 C. Chung and J. A. Burdick, *Adv. Drug Delivery Rev.*, 2008, **60**, 243–262.
- 170 K. Zwiorek, C. Bourquin, J. Battiany, G. Winter, S. Endres, G. Hartmann and C. Coester, *Pharm. Res.*, 2008, **25**, 551–562.
- 171 M. Neek, J. A. Tucker, T. I. Kim, N. M. Molino, E. L. Nelson and S.-W. Wang, *Biomaterials*, 2018, **156**, 194–203.
- 172 M. Chen, S. Gao, M. Dong, J. Song, C. Yang, K. A. Howard, J. Kjemis and F. Besenbacher, *ACS Nano*, 2012, **6**, 4835–4844.
- 173 D. M. Fan, E. De Rosa, M. B. Murphy, Y. Peng, C. A. Smid, C. Chiappini, X. W. Liu, P. Simmons, B. K. Weiner, M. Ferrari and E. Tasciotti, *Adv. Funct. Mater.*, 2012, **22**, 282–293.
- 174 M. Diwan, M. Tafaghodi and J. Samuel, *J. Controlled Release*, 2002, **85**, 247–262.
- 175 X. Wang, L. Ye, W. He, C. Teng, S. Sun, H. Lu, S. Li, L. Lv, X. Cao, H. Yin, W. Lv and H. Xin, *J. Controlled Release*, 2022, **345**, 786–797.
- 176 Q. Liu, J. Jia, T. Yang, Q. Fan, L. Wang and G. Ma, *Small*, 2016, **12**, 1744–1757.
- 177 P. Pradhan, R. Toy, N. Jhita, A. Atalis, B. Pandey, A. Beach, E. L. Blanchard, S. G. Moore, D. A. Gaul, P. J. Santangelo, D. M. Shayakhmetov and K. Roy, *Sci. Adv.*, 2021, **7**, eabd4235.
- 178 Y. Du, T. Song, J. Wu, X.-D. Gao, G. Ma, Y. Liu and Y. Xia, *Biomaterials*, 2022, **280**, 121313.
- 179 M. Mueller, W. Reichardt, J. Koerner and M. Groettrup, *J. Controlled Release*, 2012, **162**, 159–166.
- 180 Q. Liu, X. Wang, X. Liu, S. Kumar, G. Gochman, Y. Ji, Y.-P. Liao, C. H. Chang, W. Situ, J. Lu, J. Jiang, K.-C. Mei, H. Meng, T. Xia and A. E. Nel, *ACS Nano*, 2019, **13**, 4778–4794.
- 181 C. Nembrini, A. Stano, K. Y. Dane, M. Ballester, A. J. van der Vlies, B. J. Marsland, M. A. Swartz and J. A. Hubbell, *Proc. Natl. Acad. Sci. U. S. A.*, 2011, **108**, E989–E997.
- 182 A. de Titta, M. Ballester, Z. Julier, C. Nembrini, L. Jeanbart, A. J. van der Vlies, M. A. Swartz and J. A. Hubbell, *Proc. Natl. Acad. Sci. U. S. A.*, 2013, **110**, 19902–19907.
- 183 J. Cui, R. De Rose, J. P. Best, A. P. Johnston, S. Alcantara, K. Liang, G. K. Such, S. J. Kent and F. Caruso, *Adv. Mater.*, 2013, **25**, 3468–3472.
- 184 G. Kelly, J. J. Milligan, E. M. Mastria, S. Kim, S. R. Zelenetz, J. Dobbins, L. Y. Cai, X. Li, S. K. Nair and A. Chilkoti, *J. Controlled Release*, 2022, **343**, 267–276.



- 185 J. Wei, D. Wu, Y. Shao, B. Guo, J. Jiang, J. Chen, J. Zhang, F. Meng and Z. Zhong, *J. Controlled Release*, 2022, **347**, 68–77.
- 186 X. Dong, A. Yang, Y. Bai, D. Kong and F. Lv, *Biomaterials*, 2020, **230**, 119659.
- 187 J. L. Perry, S. Tian, N. Sengottuvel, E. B. Harrison, B. K. Gorentla, C. H. Kapadia, N. Cheng, J. C. Luft, J. P. Y. Ting, J. M. DeSimone and C. V. Pecot, *ACS Nano*, 2020, **14**, 7200–7215.
- 188 J. Wei, D. Wu, S. Zhao, Y. Shao, Y. Xia, D. Ni, X. Qiu, J. Zhang, J. Chen, F. Meng and Z. Zhong, *Adv. Sci.*, 2022, **9**, 2103689.
- 189 X. Song, Y. Jiang, W. Zhang, G. Elfawal, K. Wang, D. Jiang, H. Hong, J. Wu, C. He, X. Mo and H. Wang, *Acta Biomater.*, 2022, **140**, 247–260.
- 190 C. Dong, Y. Wang, W. Zhu, Y. Ma, J. Kim, L. Wei, G. X. Gonzalez and B.-Z. Wang, *ACS Appl. Mater. Interfaces*, 2022, **14**, 6331–6342.
- 191 T. Y. Shih, A. J. Najibi, A. L. Bartlett, A. W. Li and D. J. Mooney, *Biomaterials*, 2021, **279**, 121240.
- 192 H. M. Li, Y. P. Li, X. Wang, Y. Y. Hou, X. Y. Hong, T. Gong, Z. R. Zhang and X. Sun, *Theranostics*, 2017, **7**, 4383–4398.
- 193 Q. Zeng, H. Li, H. Jiang, J. Yu, Y. Wang, H. Ke, T. Gong, Z. Zhang and X. Sun, *Biomaterials*, 2017, **122**, 105–113.
- 194 K. Suzuki, Y. Yoshizaki, K. Horii, N. Murase, A. Kuzuya and Y. Ohya, *Biomater. Sci.*, 2022, **10**, 1920–1928.
- 195 Y. Xia, J. Wei, S. Zhao, B. Guo, F. Meng, B. Klumperman and Z. Zhong, *J. Controlled Release*, 2021, **336**, 262–273.
- 196 V. Guillermin, D. Kim, J. F. Eubank, R. Luebke, X. Liu, K. Adil, M. S. Lah and M. Eddaoudi, *Chem. Soc. Rev.*, 2014, **43**, 6141–6172.
- 197 Q.-L. Zhu and Q. Xu, *Chem. Soc. Rev.*, 2014, **43**, 5468–5512.
- 198 Z. Hu, B. J. Deibert and J. Li, *Chem. Soc. Rev.*, 2014, **43**, 5815–5840.
- 199 N. L. Rosi, J. Eckert, M. Eddaoudi, D. T. Vodak, J. Kim, M. Keffe and O. M. Yaghi, *Science*, 2003, **300**, 1127.
- 200 K. Wang, X.-L. Lv, D. Feng, J. Li, S. Chen, J. Sun, L. Song, Y. Xie, J.-R. Li and H.-C. Zhou, *J. Am. Chem. Soc.*, 2016, **138**, 914–919.
- 201 P. Horcajada, T. Chalati, C. Serre, B. Gillet, C. Sebrie, T. Baati, J. F. Eubank, D. Heurtaux, P. Clayette, C. Kreuz, J.-S. Chang, Y. K. Hwang, V. Marsaud, P.-N. Bories, L. Cynober, S. Gil, G. Férey, P. Couvreur and R. Gref, *Nat. Mater.*, 2010, **9**, 172–178.
- 202 H. Zheng, Y. Zhang, L. Liu, W. Wan, P. Guo, A. M. Nyström and X. Zou, *J. Am. Chem. Soc.*, 2016, **138**, 962–968.
- 203 Y. He, D. Li, L. Wu, X. Yin, X. Zhang, L. H. Patterson and J. Zhang, *Adv. Funct. Mater.*, 2023, **33**, 2212277.
- 204 S. R. Venna, J. B. Jasinski and M. A. Carreon, *J. Am. Chem. Soc.*, 2010, **132**, 18030–18033.
- 205 Y. Zhang, F. Wang, E. Ju, Z. Liu, Z. Chen, J. Ren and X. Qu, *Adv. Funct. Mater.*, 2016, **26**, 6454–6461.
- 206 H. J. Zhang, W. Chen, K. Gong and J. H. Chen, *ACS Appl. Mater. Interfaces*, 2017, **9**, 31519–31525.
- 207 O. R. Brohlin, R. N. Ehrman, F. C. Herbert, Y. H. Wijesundara, A. Raja, A. Shahrivarkevishahi, S. D. Diwakara, R. A. Smaldone and J. J. Gassensmith, *ACS Appl. Nano Mater.*, 2022, **5**, 13697–13704.
- 208 Z. Wang, Y. Fu, Z. Kang, X. Liu, N. Chen, Q. Wang, Y. Tu, L. Wang, S. Song, D. Ling, H. Song, X. Kong and C. Fan, *J. Am. Chem. Soc.*, 2017, **139**, 15784–15791.
- 209 W. Ning, Z. Di, Y. Yu, P. Zeng, C. Di, D. Chen, X. Kong, G. Nie, Y. Zhao and L. Li, *Small*, 2018, **14**, 1703812.
- 210 Y. Pang, Y. Fu, C. Li, Z. Wu, W. Cao, X. Hu, X. Sun, W. He, X. Cao, D. Ling, Q. Li, C. Fan, C. Yang, X. Kong and A. Qin, *Nano Lett.*, 2020, **20**, 829–840.
- 211 Z. Cai, F. Xin, Z. Wei, M. Wu, X. Lin, X. Du, G. Chen, D. Zhang, Z. Zhang, X. Liu and C. Yao, *Adv. Healthcare Mater.*, 2020, **9**, 1900996.
- 212 M. Eckshtain-Levi, C. J. Batty, L. M. Lifshits, B. McCammitt, K. M. Moore, E. A. Amouzougan, R. T. Stiepel, E. Duggan, T. M. Ross, E. M. Bachelder and K. M. Ainslie, *ACS Appl. Mater. Interfaces*, 2022, **14**, 28548–28558.
- 213 K. Ni, T. Luo, G. Lan, A. Culbert, Y. Song, T. Wu, X. Jiang and W. Lin, *Angew. Chem., Int. Ed.*, 2020, **59**, 1108–1112.
- 214 F. Duan, X. Feng, X. Yang, W. Sun, Y. Jin, H. Liu, K. Ge, Z. Li and J. Zhang, *Biomaterials*, 2017, **122**, 23–33.
- 215 K. Ni, G. Lan, N. Guo, A. Culbert, T. Luo, T. Wu, R. R. Weichselbaum and W. Lin, *Sci. Adv.*, 2020, **6**, eabb5223.
- 216 Z. Fan, H. Liu, Y. Xue, J. Lin, Y. Fu, Z. Xia, D. Pan, J. Zhang, K. Qiao, Z. Zhang and Y. Liao, *Bioact. Mater.*, 2021, **6**, 312–325.
- 217 X. Chen, Q. Tang, J. Wang, Y. Zhou, F. Li, Y. Xie, X. Wang, L. Du, J. Li, J. Pu, Q. Hu, Z. Gu and P. Liu, *Adv. Mater.*, 2023, **35**, 2210440.
- 218 T. M. Allen and P. R. Cullis, *Science*, 2004, **303**, 1818–1822.
- 219 V. Wagner, A. Dullaart, A.-K. Bock and A. Zweck, *Nat. Biotechnol.*, 2006, **24**, 1211–1217.
- 220 S. Inturi, G. Wang, F. Chen, N. K. Banda, V. M. Holers, L. Wu, S. M. Moghimi and D. Simberg, *ACS Nano*, 2015, **9**, 10758–10768.
- 221 K. Yi, H. Kong, C. Zheng, C. Zhuo, Y. Jin, Q. Zhong, R. L. Mintz, E. Ju, H. Wang, S. Lv, Y.-H. Lao, Y. Tao and M. Li, *Biomaterials*, 2023, **302**, 122349.
- 222 H. Kong, C. Zhuo, K. Yi, C. Zheng, R. L. Mintz, Y.-H. Lao, Q. Zhong, E. Ju, H. Wang, D. Shao, H. Xiao, Y. Tao and M. Li, *Nano Today*, 2023, **53**, 102040.
- 223 C. Zheng, Q. Zhong, W. Song, K. Yi, H. Kong, H. Wang, Y. Tao, M. Li and X. Chen, *Adv. Mater.*, 2023, **35**, 2206989.
- 224 C. Zheng, Q. Zhong, K. Yi, H. Kong, F. Cao, C. Zhuo, Y. Xu, R. Shi, E. Ju, W. Song, Y. Tao, X. Chen and M. Li, *Sci. Adv.*, 2023, **9**, eadh2413.
- 225 Y. Matsumura and H. Maeda, *Cancer Res.*, 1986, **46**, 6387–6392.
- 226 Q. Su, C. Wang, H. Song, C. Zhang, J. Liu, P. Huang, Y. Zhang, J. Zhang and W. Wang, *J. Mater. Chem. B*, 2021, **9**, 3892–3899.
- 227 W. M. Li, W. H. Dragowska, M. B. Bally and M.-P. Schutze-Redelmeier, *Vaccine*, 2003, **21**, 3319–3329.
- 228 Y. Yoshizaki, E. Yuba, N. Sakaguchi, K. Koiwai, A. Harada and K. Kono, *Biomaterials*, 2017, **141**, 272–283.

- 229 J.-O. Jin, H. Kim, Y. H. Huh, A. Herrmann and M. Kwak, *J. Controlled Release*, 2019, **315**, 76–84.
- 230 L. Munakata, Y. Tanimoto, A. Osa, J. Meng, Y. Haseda, Y. Naito, H. Machiyama, A. Kumanogoh, D. Omata, K. Maruyama, Y. Yoshioka, Y. Okada, S. Koyama, R. Suzuki and T. Aoshi, *J. Controlled Release*, 2019, **313**, 106–119.
- 231 C. H. Lai, S. L. Duan, F. Ye, X. Q. Hou, X. Li, J. Zhao, X. Yu, Z. X. Hu, Z. R. Tang, F. Z. Mo, X. M. Yang and X. L. Lu, *Theranostics*, 2018, **8**, 1723–1739.
- 232 H. Zhao, B. Zhao, L. Wu, H. Xiao, K. Ding, C. Zheng, Q. Song, L. Sun, L. Wang and Z. Zhang, *ACS Nano*, 2019, **13**, 12553–12566.
- 233 J. Meng, P. Zhang, Q. Chen, Z. Wang, Y. Gu, J. Ma, W. Li, C. Yang, Y. Qiao, Y. Hou, L. Jing, Y. Wang, Z. Gu, L. Zhu, H. Xu, X. Lu and M. Gao, *Adv. Mater.*, 2022, **34**, 2202168.
- 234 N. M. Molino, A. K. Anderson, E. L. Nelson and S. W. Wang, *ACS Nano*, 2013, **7**, 9743–9752.
- 235 N. Butkovich, J. A. Tucker, A. Ramirez, E. Li, V. S. Meli, E. L. Nelson and S.-W. Wang, *Biomater. Sci.*, 2023, **11**, 596–610.
- 236 R. Kuai, L. J. Ochyl, K. S. Bahjat, A. Schwendeman and J. J. Moon, *Nat. Mater.*, 2017, **16**, 489.
- 237 G. Zhu, G. M. Lynn, O. Jacobson, K. Chen, Y. Liu, H. Zhang, Y. Ma, F. Zhang, R. Tian, Q. Ni, S. Cheng, Z. Wang, N. Lu, B. C. Yung, Z. Wang, L. Lang, X. Fu, A. Jin, I. D. Weiss, H. Vishwasrao, G. Niu, H. Shroff, D. M. Klinman, R. A. Seder and X. Chen, *Nat. Commun.*, 2017, **8**, 1954.
- 238 H. Zhang, L. Lai, Y. Wang, B. Ye, S. Deng, A. Ding, L. Teng, L. Qiu and J. Chen, *ACS Biomater. Sci. Eng.*, 2019, **5**, 6082–6088.
- 239 A. K. Kozłowska, A. Florczak, M. Smialek, E. Dondajewska, A. Mackiewicz, M. Kortylewski and H. Dams-Kozłowska, *Acta Biomater.*, 2017, **59**, 221–233.
- 240 X. Shi, H. Song, C. Wang, C. Zhang, P. Huang, D. Kong, J. Zhang and W. Wang, *Chem. Eng. J.*, 2020, **399**, 125854.
- 241 D. Qiao, L. Li, L. Liu and Y. Chen, *ACS Appl. Mater. Interfaces*, 2022, **14**, 50592–50600.
- 242 B. Zhang, X. Chen, G. Tang, R. Zhang, J. Li, G. Sun, X. Yan and K. Fan, *Nano Today*, 2022, **46**, 101564.
- 243 M. A. Scully, E. H. Sterin and E. S. Day, *Biomater. Sci.*, 2022, **10**, 4378–4391.
- 244 M. Morishita, Y. Takahashi, A. Matsumoto, M. Nishikawa and Y. Takakura, *Biomaterials*, 2016, **111**, 55–65.
- 245 W. Liu, M. Ota, M. Tabushi, Y. Takahashi and Y. Takakura, *J. Controlled Release*, 2022, **345**, 433–442.
- 246 G. Zhao, H. Liu, Z. Wang, H. Yang, H. Zhao, Y. Zhang, K. Ge, X. Wang, L. Luo, X. Zhou, J. Zhang and Z. Li, *Acta Biomater.*, 2022, **153**, 529–539.
- 247 Z. Fan, Y. Wang, L. Li, F. Zeng, Q. Shang, Y. Liao, C. Liang and L. Nie, *ACS Nano*, 2022, **16**, 16177–16190.
- 248 J. Cui, X. Wang, J. Li, A. Zhu, Y. Du, W. Zeng, Y. Guo, L. Di and R. Wang, *ACS Nano*, 2023, **17**, 1464–1484.
- 249 A. V. Kroll, R. H. Fang, Y. Jiang, J. Zhou, X. Wei, C. L. Yu, J. Gao, B. T. Luk, D. Dehaini, W. Gao and L. Zhang, *Adv. Mater.*, 2017, **29**, 1703969.
- 250 M. Holay, N. Krishnan, J. Zhou, Y. Duan, Z. Guo, W. Gao, R. H. Fang and L. Zhang, *Nano Lett.*, 2022, **22**, 9672–9678.
- 251 S. Liu, J. Wu, Y. Feng, X. Guo, T. Li, M. Meng, J. Chen, D. Chen and H. Tian, *Bioact. Mater.*, 2023, **22**, 211–224.
- 252 J. Wang, B. Sun, L. Sun, X. Niu, L. Li and Z. P. Xu, *Biomater. Sci.*, 2023, **11**, 2020–2032.
- 253 C. Yang, Y. He, F. Chen, F. Zhang, D. Shao and Z. Wang, *Small*, 2023, **9**, 2207029.
- 254 L. K. M. Lam, S. Murphy, D. Kokkinaki, A. Venosa, S. Sherrill-Mix, C. Casu, S. Rivella, A. Weiner, J. Park, S. Shin, A. E. Vaughan, B. H. Hahn, A. R. Odom John, N. J. Meyer, C. A. Hunter, G. S. Worthen and N. S. Mangalmurti, *Sci. Transl. Med.*, 2021, **13**, eabj1008.